NMR analysis of the backbone dynamics of the small GTPase Rheb and its interaction with the regulatory protein FKBP38

Maristella De Cicco[1], Leo Kiss[1,2], and Sonja A. Dames[1,3§]

[1]Technische Universität München, Department of Chemistry, Biomolecular NMR Spectroscopy, Lichtenbergstr. 4, 85747 Garching, Germany

[2]Current Affiliation: Institute of Pharmacy and Molecular Biotechnology, Heidelberg University, 69120 Heidelberg, Germany

[3]Institute of Structural Biology, Helmholtz Zentrum München, Ingolstädter Landstr. 1, 85764 Neuherberg, Germany

[§]To whom correspondence may be addressed. E-mail: sonja.dames@tum.de

Supplementary Information

Supplementary Results

Comparison of the backbone dynamics of two different GTP analogue-bound states of RhebΔCT.

The backbone dynamic behavior of RhebΔCT bound to GTP-analogues RhebΔCT-GppNHp and –GppCp is overall similar (SI Fig. S4). The average ^{15}N-T_1, -T_2, and {^{1}H}-^{15}N NOE values for RhebΔCT-GppCp are 725 ± 77 ms and 94 ± 21 ms, and 0.77 ± 0.14, respectively compared to 716 ± 41 ms 87 ± 17 ms, and 0.79 ± 0.11, respectively for the GppNHp-bound state. The values for all analyzable residues for the GppCp-bound state are listed in SI table S3. Differences to the GppNHp-bound state were generally observed for residues involved in nucleotide-binding (based on Uniprot-ID Q15382: 16-21 in G1/P-loop, 32-38 in G2/switch 1, 119-122 in G4, 149-150 in G5) or spatially close to the nucleotide binding region. This include residues near the β and γ phosphate group of the nucleotide, i. e. in the P-loop T14, K19 and S20, and several residues in as well as between the G4 and G5 regions. In addition, the conformational differences due to the different chemical bond between the β and γ phosphate group of the nucleotide appeared to slightly modulate the dynamics of residues in the two β-strands following the switch 1 region (≈ residues 45-55) and the loop region around residues 85-90 that is spatially close to the nucleotide binding region.

Supplementary Tables

Supplementary Table S1: ^{15}N-relaxation times T_1 and T_2, and {^{1}H}-^{15}N NOE values and corresponding errors for the GDP-bound form of RhebΔCT

Residue	^{15}N-T_1 [ms] ± error	^{15}N-T_2 [ms] ± error	{^{1}H}-^{15}N NOE ± error
6	724 ± 2	100 ± 0	0.70 ± 0.03
7	673 ± 1	95 ± 0	0.80 ± 0.03
8	690 ± 1	100 ± 1	0.81 ± 0.03
9	641 ± 1	100 ± 1	0.76 ± 0.03
10	614 ± 1	94 ± 1	0.81 ± 0.04
11	655 ± 1	91 ± 1	0.74 ± 0.03
12	651 ± 1	88 ± 1	0.75 ± 0.03
14	666 ± 2	88 ± 1	0.78 ± 0.04
15	657 ± 5	96 ± 1	0.87 ± 0.10
16	677 ± 2	81 ± 1	0.80 ± 0.04
18	616 ± 2	87 ± 1	0.78 ± 0.04
19	677 ± 3	86 ± 1	0.92 ± 0.05
20	694 ± 2	76 ± 0	0.86 ± 0.03
21	729 ± 2	78 ± 1	0.92 ± 0.03
22	650 ± 1	85 ± 0	0.85 ± 0.02
24	665 ± 2	78 ± 0	0.85 ± 0.03
25	651 ± 2	84 ± 0	0.93 ± 0.04
26	663 ± 2	79 ± 0	0.91 ± 0.03
27	670 ± 1	77 ± 0	0.83 ± 0.03
28	698 ± 2	80 ± 1	0.80 ± 0.03
29	644 ± 2	90 ± 0	0.83 ± 0.04
31	721 ± 1	95 ± 0	0.74 ± 0.03
32	720 ± 2	96 ± 0	0.74 ± 0.05
33	670 ± 1	108 ± 0	0.71 ± 0.02
34	671 ± 1	114 ± 0	0.73 ± 0.03

35	694 ± 1	143 ± 0	0.48 ± 0.03
36	764 ± 4	103 ± 1	0.78 ± 0.04
38	684 ± 2	81 ± 1	0.78 ± 0.03
39	640 ± 6	85 ± 0	0.62 ± 0.08
40	668 ± 1	86 ± 1	0.78 ± 0.06
41	755 ± 2	86 ± 1	0.71 ± 0.03
42	726 ± 2	76 ± 0	0.86 ± 0.04
43	654 ± 2	78 ± 1	0.76 ± 0.03
44	717 ± 1	85 ± 0	0.82 ± 0.03
45	665 ± 1	81 ± 0	0.75 ± 0.03
46	703 ± 1	78 ± 0	0.81 ± 0.02
47	675 ± 1	84 ± 0	0.78 ± 0.03
48	692 ± 1	79 ± 0	0.83 ± 0.03
51	769 ± 4	80 ± 1	0.81 ± 0.02
52	745 ± 1	90 ± 0	0.77 ± 0.03
53	735 ± 1	84 ± 1	0.74 ± 0.03
54	667 ± 1	95 ± 0	0.82 ± 0.03
55	693 ± 1	96 ± 0	0.82 ± 0.03
56	670 ± 1	108 ± 0	0.77 ± 0.03
57	662 ± 1	114 ± 0	0.78 ± 0.03
58	655 ± 1	143 ± 0	0.83 ± 0.03
59	667 ± 1	103 ± 1	0.84 ± 0.04
60	701 ± 2	97 ± 1	0.70 ± 0.07
61	677 ± 4	103 ± 1	0.85 ± 0.03
62	708 ± 1	90 ± 0	0.58 ± 0.05
63	664 ± 2	118 ± 1	0.85 ± 0.08
64	634 ± 3	90 ± 1	0.87 ± 0.03
65	720 ± 2	86 ± 0	0.84 ± 0.05
66	718 ± 3	88 ± 1	0.76 ± 0.03
68	668 ± 1	86 ± 0	0.78 ± 0.03
69	708 ± 2	89 ± 0	0.79 ± 0.04
74	609 ± 2	73 ± 0	0.77 ± 0.03
75	609 ± 1	92 ± 0	0.80 ± 0.04

76	680 ± 3	92 ± 0	0.45 ± 0.05
77	670 ± 1	71 ± 0	0.78 ± 0.05
78	669 ± 2	92 ± 0	0.81 ± 0.05
79	666 ± 1	89 ± 1	0.76 ± 0.03
83	664 ± 1	93 ± 0	0.72 ± 0.03
84	647 ± 1	92 ± 1	0.77 ± 0.03
85	650 ± 1	87 ± 1	0.87 ± 0.03
86	701 ± 2	89 ± 1	0.80 ± 0.04
87	682 ± 1	74 ± 0	0.79 ± 0.03
88	675 ± 2	85 ± 0	0.91 ± 0.04
89	673 ± 1	79 ± 0	0.83 ± 0.02
90	660 ± 1	85 ± 0	0.83 ± 0.03
91	643 ± 1	87 ± 0	0.92 ± 0.02
92	675 ± 1	83 ± 0	0.83 ± 0.03
93	639 ± 2	85 ± 0	0.78 ± 0.04
94	701 ± 1	80 ± 0	0.87 ± 0.03
95	660 ± 1	81 ± 0	0.84 ± 0.03
96	64 ± 1	68 ± 0	0.86 ± 0.04
97	650 ± 4	72 ± 0	0.81 ± 0.07
98	674 ± 3	86 ± 1	0.76 ± 0.06
99	687 ±1	83 ± 0	0.82 ± 0.03
101	656 ± 3	77 ± 0	0.82 ± 0.05
105	688 ± 1	82 ± 0	0.78 ± 0.03
106	100 ± 1	89 ± 0	0.74 ± 0.03
107	686 ± 1	89 ± 0	0.77 ± 0.03
108	672 ± 1	96 ± 0	0.75 ± 0.03
109	733 ± 2	109 ± 1	0.66 ± 0.04
110	729 ± 1	133 ± 0	0.43 ± 0.03
111	736 ±1	122 ± 0	0.56 ± 0.03
112	771 ± 1	125 ± 0	0.43 ± 0.03
115	647 ± 1	95 ± 1	0.74 ± 0.03
116	647 ± 1	93 ± 1	0.89 ± 0.03
118	659 ± 2	90 ± 1	0.83 ± 0.04

119	661 ± 1	85 ± 1	0.78 ± 0.02
120	746 ± 6	84 ± 1	0.95 ± 0.08
121	685 ± 1	79 ± 0	0.78 ± 0.03
122	622 ± 1	80 ± 0	0.86 ± 0.03
123	692 ± 2	90 ± 0	0.89 ± 0.04
124	665 ± 2	88 ± 0	0.79 ± 0.03
125	735 ± 2	85 ± 1	0.74 ± 0.03
127	647 ± 3	87 ±	0.75 ± 0.05
128	670 ± 2	79 ± 1	0.86 ± 0.05
129	690 ± 3	98 ± 1	0.81 ± 0.05
130	694 ± 1	88 ± 0	0.84 ± 0.03
131	654 ± 2	88 ± 0	0.88 ± 0.03
132	683 ± 1	83 ± 0	0.88 ± 0.02
133	691 ± 1	85 ± 0	0.80 ± 0.03
134	654 ± 3	93 ± 1	0.74 ± 0.6
135	649 ± 2	83 ± 0	0.85 ± 0.03
136	658 ± 1	79 ± 0	0.84 ± 0.03
137	610 ± 3	88 ± 0	0.74 ± 0.05
138	649 ± 1	82 ± 0	0.86 ± 0.03
139	676 ± 1	80 ± 0	0.83 ± 0.02
140	650 ± 1	80 ± 0	0.80 ± 0.03
141	677 ± 2	94 ± 1	0.75 ± 0.04
142	711 ± 1	82 ± 0	0.44 ± 0.07
143	714 ± 1	81 ± 0	0.86 ± 0.03
144	720 ± 1	100 ± 0	0.73 ± 0.03
145	685 ± 1	93 ± 0	0.87 ± 0.03
146	653 ± 2	89 ± 0	0.86 ± 0.03
147	678 ± 2	93 ± 0	0.78 ± 0.04
148	666 ± 1	83 ± 1	0.91 ± 0.03
149	737 ± 2	84 ± 0	0.85 ± 0.04
150	689 ± 1	90 ± 0	0.90 ± 0.03
151	660 ± 3	86 ± 0	0.79 ± 0.05
152	660 ± 2	90 ± 0	0.78 ± 0.04

154	753 ± 2	88 ± 0	0.83 ± 0.03
155	646 ± 3	96 ± 0	0.81 ± 0.05
156	654 ± 1	93 ± 0	0.86 ± 0.05
157	677 ± 1	82 ± 0	0.76 ± 0.02
158	654 ± 3	81 ± 0	0.83 ± 0.02
159	650 ± 5	82 ± 0	0.77 ± 0.05
160	661 ± 1	83 ± 1	0.77 ± 0.10
161	686 ± 5	83 ± 0	0.82 ± 0.02
163	626 ± 5	82 ± 0	0.70 ± 0.03
164	684 ± 1	81 ± 1	0.83 ± 0.08
165	637 ± 1	82 ± 0	0.72 ± 0.03
166	657 ± 1	83 ± 0	0.81 ± 0.03
167	649 ± 1	94 ± 0	0.81 ± 0.02
168	649 ± 1	95 ± 0	0.67 ± 0.03
169	606 ± 0	117 ± 0	0.50 ± 0.02
170	614 ± 0	194 ± 0	0.37 ± 0.02

Supplementary Table S2: ^{15}N-relaxation times T_1 and T_2, and {^{1}H}-^{15}N NOE values and corresponding errors for the GppNHp-bound form of RhebΔCT

Residue	^{15}N-T_1 [ms] ± error	^{15}N-T_2 [ms] ± error	{^{1}H}-^{15}N NOE ± error
4	87± 3	170 ± 1	0.12 ± 0.06
5	773 ± 3	124 ± 1	0.39 ± 0.06
6	756 ± 1	94 ± 0	0.74 ± 0.04
7	709 ± 1	95 ± 0	0.86 ± 0.05
8	702 ± 1	93 ± 0	0.81 ± 0.05
9	668 ± 1	88 ± 0	0.74 ± 0.05
10	696 ± 2	93 ± 1	0.69 ± 0.07
11	671 ± 1	87 ± 0	0.77 ± 0.06
12	725 ± 1	90 ± 0	0.84 ± 0.05
13	682 ± 1	97 ± 0	0.78 ± 0.05
14	655 ± 2	80 1	0.89 ± 0.10
16	638 ± 1	79 ± 0	0.88 ± 0.07
17	675 ± 2	95 ± 0	0.77 ± 0.06

18	828 ± 3	88 ± 1	0.82 ± 0.08
20	710 ± 3	73 ± 0	0.79 ± 0.05
21	728 ± 2	68 ± 1	0.87 ± 0.10
22	715 ± 1	85 ± 1	0.81 ± 0.06
23	794 ± 6	77 ± 0	0.86 ± 0.05
26	697 ± 1	75 ± 0	0.82 ± 0.04
27	732 ± 1	75 ± 0	0.78 ± 0.06
28	698 ± 1	73 ± 0	0.78 ± 0.05
29	698 ± 1	91 ± 0	0.88 ± 0.05
43	695 ± 2	77 ± 1	0.81 ± 0.07
44	708 ± 1	91 ± 0	0.30 ± 0.04
45	705 ± 1	88 ± 0	0.77 ± 0.04
46	724 ± 1	99 ± 0	0.76 ± 0.04
47	708 ± 1	83 ± 0	0.76 ± 0.03
48	760 ± 1	94 ± 0	0.81 ± 0.03
49	735 ± 1	97 ± 0	0.75 ± 0.04
51	823 ± 1	98 ± 0	0.70 ± 0.04
52	804 ± 1	82 ± 0	0.74 ± 0.03
53	764 ± 1	92 ± 0	0.73 ± 0.03
54	755 ± 1	87 ± 0	0.69 ± 0.04
55	734 ± 1	90 ± 0	0.78 ± 0.04
56	689 ± 1	89 ± 0	0.71 ± 0.05
57	698 ± 1	87 ± 0	0.73 ± 0.06
58	699 ± 1	93 ± 0	0.86 ± 0.06
59	674 ± 1	91 ± 0	0.88 ± 0.06
63	827 ± 6	82 ± 1	0.96 ± 0.13
65	775 ± 1	91 ± 0	0.71 ± 0.04
66	733 ± 4	81 ± 1	0.72 ± 0.16
67	684 ± 1	81 ± 0	0.85 ± 0.04
68	781 ± 1	87 ± 0	0.80 ± 0.03
77	713 ± 2	91 ± 1	0.77 ± 0.10
79	695 ± 1	90 ± 0	0.67 ± 0.06
80	661 ± 1	100 ± 0	0.65 ± 0.05

81	690 ± 1	81± 0	0.88 ± 0.06
82	654± 1	85 ± 0	0.77 ± 0.05
83	668 ± 1	94 ± 0	0.84 ± 0.05
84	693 ± 1	89 ± 0	0.90 ± 0.05
85	670 ± 1	81 ± 0	0.87 ± 0.05
86	692 ± 2	83 ± 0	0.98 ± 0.08
87	702 ± 1	66 ± 0	0.89± 0.05
88	721 ± 1	80 ± 0	0.84 ± 0.05
90	702 ± 1	86 ± 0	0.79 ± 0.05
92	695 ± 1	86 ± 0	0.85 ± 0.04
93	714 ± 1	84 ± 0	0.86 ± 0.05
94	699 ± 1	78 ± 0	0.85 ± 0.04
95	708 ± 1	79 ± 0	0.80 ± 0.04
96	717 ± 1	72 ± 0	0.77 ± 0.04
97	673 ± 1	79 ± 0	0.77 ± 0.06
98	678 ± 1	75 ± 0	0.92 ± 0.05
99	710 ± 1	74 ± 0	0.80 ± 0.05
100	782 ± 1	71 ± 0	0.84 ± 0.04
101	692 ± 1	80 ± 0	0.98 ± 0.06
102	732 ± 1	79 ± 0	0.85 ± 0.04
107	744 ± 1	79 ± 0	0.66 ± 0.04
108	752 ± 1	102 ± 0	0.66 ± 0.04
109	774 ± 2	91 ± 1	0.72 ± 0.10
110	801 ± 1	129 ± 0	0.44 ± 0.03
111	725 ± 1	119± 0	0.54 ± 0.04
112	805 ± 0	124 ± 0	0.40 ± 0.03
114	701 ± 1	93 ± 0	0.73 ± 0.05
115	668 ± 1	87 ± 0	0.74 ± 0.04
116	653 ± 1	96 ± 0	0.73 ± 0.05
117	651 ± 1	90 ± 0	0.82 ± 0.04
118	734 ± 2	83 ± 0	0.97 ± 0.06
119	687 ± 1	84 ± 0	0.82 ± 0.03
120	732 ± 2	84 ± 0	0.81 ± 0.07

121	723 ± 1	74 ± 0	0.90 ± 0.04
122	647 ± 1	77 ± 0	0.92 ± 0.05
123	704 ± 1	82 ± 0	0.93 ± 0.04
124	738 ± 1	85 ± 0	0.81 ± 0.03
126	748 ± 1	85 ± 0	0.70 ± 0.04
127	692 ± 1	85 ± 0	0.83 ± 0.05
128	681 ± 2	70 ± 1	0.86 ± 0.08
129	712 ± 1	96 ± 0	0.73 ± 0.06
130	742 ± 1	88 ± 0	0.79 ± 0.04
131	724 ± 1	86 ± 0	0.82 ± 0.04
132	736 ± 1	82 ± 0	0.86 ± 0.03
133	724 ± 1	79 ± 0	0.81 ± 0.04
134	682 ± 1	91 ± 0	0.85 ± 0.05
135	707 ± 1	76 ± 0	0.84 ± 0.04
136	718 ± 1	76 ± 0	0.84 ± 0.03
137	679 ± 1	75 ± 0	0.81 ± 0.04
138	706 ± 1	80 ± 0	0.86 ± 0.04
139	710 ± 0	76 ± 0	0.83 ± 00.3
140	748 ± 1	78 ± 0	0.81 ± 0.03
141	732 ± 1	88 ± 0	0.85 ± 0.04
142	745 ± 1	76 ± 0	0.81 ± 0.03
143	742 ± 1	78 ± 0	0.77 ± 0.03
144	753 ± 1	99 ± 0	0.71 ± 0.03
145	720 ± 1	88 ± 0	0.90 ± 0.04
146	709 ± 1	84 ± 0	0.79 ± 0.03
147	729 ± 1	89 ± 0	0.77 ± 0.03
148	700 ± 1	79 ± 0	0.80 ± 0.04
149	777 ± 1	84 ± 0	0.84 ± 0.05
150	705 ± 1	86 ± 0	0.91 ± 0.05
151	716 ± 1	84 ± 0	0.79 ± 0.06
152	718 ± 1	82 ± 0	0.81 ± 0.04
154	727 ± 2	84 ± 0	0.76 ± 0.04
155	693 ± 1	80 ± 0	0.76 ± 0.05

156	707 ± 1	89 ± 0	0.77 ± 0.04
157	720 ± 1	80 ± 0	0.81 ± 0.04
158	713 ± 1	77 ± 0	0.85 ± 0.03
159	693 ± 1	77 ± 0	0.85 ± 0.04
160	644 ± 2	82 ± 0	0.89 ± 0.07
162	692 ± 1	75 ± 0	0.80 ± 0.04
164	706 ± 1	80 ± 0	0.83 ± 0.06
165	690 ± 1	78 ± 0	0.75 ± 0.04
166	699 ± 1	83 ± 0	0.79 ± 0.03
167	696 ± 0	84 ± 0	0.82 ± 0.03
168	723 ± 0	87 ± 0	0.73 ± 0.02
169	683 ± 0	98 ± 0	0.60 ± 0.01
170	660 ± 0	186 ± 0	0.38 ± 0.02

Supplementary Table S3: ^{15}N-relaxation times T_1 and T_2, and {^{1}H}-^{15}N NOE values and corresponding errors for the GppCp-bound form of RhebΔCT

Residue	^{15}N-T_1 [ms] ± error	^{15}N-T_2 [ms] ± error	{^{1}H}-^{15}N NOE ± error
5	863 ± 7	151 ± 3	0.58 ± 0.12
6	746 ± 4	105 ± 1	0.73 ± 0.08
7	657 ± 3	85 ± 2	0.77 ± 0.09
8	725 ± 5	118 ± 3	0.91 ± 0.13
9	806 ± 7	104 ± 3	0.82 ± 0.12
10	680 ± 4	105 ± 3	0.86 ± 0.15
11	672 ± 4	92 ± 3	0.81 ± 0.13
13	640 ± 6	113 ± 3	0.67 ± 0.13
14	857 ± 12	83 ± 3	0.62 ± 0.13
17	644 ± 3	99 ± 2	0.76 ± 0.13
18	606 ±5	103 ± 3	0.79 ± 0.11
20	804 ± 7	70 ± 1	0.65 ± 0.12
22	731± 4	78 ± 1	0.73 ± 0.12
23	763 ± 5	77 ± 1	0.78 ± 0.13
26	665 ± 5	73 ± 2	0.92 ± 0.09
29	656 ± 3	115 ± 3	0.79 ± 0.11

44	815 ± 4	92 ± 2	0.73 ± 0.09
46	767 ± 4	116 ± 2	0.83 ± 0.13
47	716 ± 3	85 ± 1	0.71 ± 0.09
49	750 ± 4	113 ± 3	0.75 ± 0.10
52	773 ± 4	93 ± 1	0.76 ± 0.14
53	747 ± 3	93 ± 1	0.60 ± 0.12
54	694 ± 4	117 ± 3	0.70 ± 0.14
55	733 ± 6	94 ± 2	0.91 ± 0.13
56	718 ± 5	92 ± 2	0.94 ± 0.13
58	627 ± 5	104 ± 3	0.83 ± 0.13
59	682 ± 5	95 ± 2	0.79 ± 0.12
79	623 ± 4	92 ± 3	0.75 ± 0.12
80	678 ± 4	104 ± 2	0.70 ± 0.12
81	722 ± 6	79 ± 2	0.89 ± 0.12
82	596 ± 3	102 ± 3	0.77 ± 0.13
85	788 ± 8	90 ± 2	0.63 ± 0.11
87	681 ± 7	70 ± 1	0.89 ± 0.12
88	621 ± 4	95 ± 2	0.75 ± 0.11
90	852 ± 5	105 ± 3	0.89 ± 0.11
93	738 ± 6	94	0.71 ± 0.11
94	697 ± 3	91 ± 2	0.79 ± 0.10
95	722 ± 4	103 ± 2	0.93 ± 0.17
96	735 ± 4	66 ± 1	0.72 ± 0.13
97	611 ± 5	69 ± 2	0.86 ± 0.12
98	699 ± 4	83 ± 2	0.93 ± 0.11
99	750 ± 5	89 ± 2	0.82 ± 0.09
101	610 ± 3	102 ± 2	0.75 ± 0.10
102	709 ± 4	80 ± 2	0.77 ± 0.10
103	690 ± 4	78 ± 1	0.99 ± 0.08
105	810 ± 6	90 ± 2	0.66 ± 0.07
107	732 ± 3	82 ± 1	0.86 ± 0.07
108	743 ± 3	96 ± 1	0.81 ± 0.08
109	782 ± 5	103 ± 2	0.86 ± 0.13

110	764 ± 2	139 ± 1	0.52 ± 0.13
111	805 ± 5	127 ± 3	0.44 ± 0.15
112	767 ± 2	119 ± 1	0.36 ± 0.11
114	753 ± 3	111 ± 1	0.89 ± 0.10
115	805 ± 5	94 ± 2	0.78 ± 0.11
116	730 ± 7	106 ± 4	0.80 ± 0.08
117	703 ± 5	103 ± 3	0.77 ± 0.16
120	672 ± 9	69 ± 2	0.68 ± 0.13
121	685 ± 4	69 ± 1	0.90 ± 0.08
122	755 ± 5	93 ± 2	1.02 ± 0.07
123	631 ± 4	84 ± 1	0.95 ± 0.09
124	737 ± 4	79 ± 1	0.79 ± 0.12
125	406 ± 17	85 ± 1	0.71 ± 0.10
126	792 ± 4	80 ± 1	0.77 ± 0.08
127	954 ± 10	91 ± 2	0.61 ± 0.12
128	787 ± 6	69 ± 1	0.69 ± 0.10
129	798 ± 7	74 ± 2	0.76 ± 0.10
132	802 ± 4	89 ± 1	0.87 ± 0.07
133	657 ± 3	78 ± 1	0.84 ± 0.10
134	698 ± 6	102 ± 2	0.69 ± 0.07
135	752 ± 4	82 ± 1	0.87 ± 0.11
136	715 ± 3	81 ± 1	0.70 ± 0.10
137	861 ± 6	87 ± 1	0.92 ± 0.11
138	725 ± 3	80 ± 2	0.89 ± 0.11
139	861 ± 6	75 ± 1	0.90 ± 0.10
140	725 ± 3	78 ± 1	0.80 ± 0.16
141	765 ± 3	91 ± 2	0.69 ± 0.11
143	728 ± 5	69 ± 1	0.74 ± 0.11
144	836 ± 4	105 ± 1	0.91 ± 0.09
145	781 ± 4	85 ± 1	0.98 ± 0.12
146	747 ± 3	87 ± 2	0.89 ± 0.10
148	621 ± 2	113 ± 3	0.83 ± 0.08
149	711 ± 3	96 ± 2	0.83 ± 0.13

150	778 ± 6	99 ± 2	0.81 ± 0.20
152	729 ± 4	81 ± 1	0.85 ± 0.07
154	741 ± 4	89 ± 1	0.69 ± 0.16
155	759 ± 5	89 ± 2	0.86 ± 0.09
156	608 ± 4	81 ± 1	0.90 ± 0.08
157	673 ± 3	84 ± 2	0.74 ± 0.06
158	799 ± 3	80 ± 1	0.80 ± 0.04
159	732 ± 4	71 ± 1	0.82 ± 0.06
162	736 ± 4	93 ± 2	0.77 ± 0.00
164	699 ± 8	80 ± 2	0.80 ± 0.01
165	681 ± 3	80 ± 1	0.78 ± 0.12
166	672 ± 4	132 ± 3	0.68 ± 0.08
167	698 ± 2	94 ± 1	0.69 ± 0.09
168	678 ± 1	84 ± 1	0.72 ± 0.13
169	667 ± 1	99 ± 0	0.58 ± 0.12
170	638 ± 1	192 ± 1	0.29 ± 0.15

Supplementary Table S4: ^{15}N-relaxation times T_1 and T_2, and {^{1}H}-^{15}N NOE values and corresponding errors for the GppNHp-bound form of RhebΔCT in the presence of FKBP38-BD

Residue	^{15}N-T_1[ms] ± error	^{15}N-T_2 [ms] ± error	{^{1}H}-^{15}N NOE ± error
4	726 ± 2	170 ± 0	0.43 ± 0.08
5	663 ± 2	118 ± 0	0.67 ± 0.10
6	771 ± 2	93 ± 0	0.69 ± 0.06
7	710 ± 2	88 ± 1	0.80 ± 0.06
8	755 ± 2	93 ± 1	0.89 ± 0.06
9	720 ± 2	90 ± 1	0.84 ± 0.07
10	700 ± 3	106 ± 1	0.81 ± 0.08
12	665 ± 2	89 ± 1	0.84 ± 0.07
13	756 ± 3	97 ± 1	0.80 ± 0.07
14	718 ± 8	98 ± 2	0.92 ± 0.12
16	795 ± 6	88 ± 1	0.73 ± 0.09
17	570 ± 2	84 ± 1	1.08 ± 0.08
18	574 ± 4	77 ± 1	1.01 ± 0.11

20	705 ± 3	75 ± 1	0.73 ± 0.07
21	844 ± 7	75 ± 2	0.84 ± 0.12
22	620 ± 3	87 ± 1	0.69 ± 0.07
23	728 ± 3	71 ± 1	0.90 ± 0.07
24	717 ± 3	60 ± 1	0.59 ± 0.08
25	704 ± 1	74 ± 0	0.92 ± 0.05
26	706 ± 2	76 ± 0	0.78 ± 0.05
27	719 ± 3	74 ± 1	0.81 ± 0.08
28	707 ± 2	90 ± 1	0.95 ± 0.07
29	688 ± 2	117 ± 5	0.66 ± 0.06
44	777 ± 1	91 ± 0	0.91 ± 0.05
46	703 ± 1	97 ± 1	0.77 ± 0.06
47	672 ± 1	85± 0	0.83 ± 0.05
48	713 ± 1	92 ± 0	0.81 ± 0.04
49	711 ± 2	90 ± 0	0.68 ± 0.05
51	801 ± 3	95 ± 0	0.85 ± 0.08
52	820 ± 2	81 ± 0	0.68 ± 0.04
53	717 ± 1	87 ± 0	0.74 ± 0.05
54	693 ± 2	86 ± 0	0.70 ± 0.07
56	689 ± 2	85 ± 1	0.78 ± 0.04
57	686 ± 3	92 ± 1	0.73 ± 0.07
58	588 ± 2	85 ± 1	0.87 ± 0.08
59	652 ± 2	91 ± 1	0.81 ± 0.08
63	770 ± 8	86 ± 2	0.84 ± 0.07
65	703 ± 2	88 ± 1	0.77 ± 0.07
67	645 ± 2	76 ± 0	0.67 ± 0.05
68	722 ± 2	88 ± 0	0.86 ± 0.03
78	786 ± 4	90 ± 1	0.75 ± 0.07
79	669 ± 2	81 ± 1	0.69 ± 0.06
84	655 ± 2	81 ± 1	0.83 ± 0.07
85	635 ± 2	76 ± 1	0.83 ± 0.06
86	763 ± 5	79 ± 1	0.90 ± 0.10
87	691 ± 2	68 ± 0	0.86 ± 0.06

88	701 ± 2	76 ± 0	0.82 ± 0.06
90	686 ± 2	80 ± 0	0.83 ± 0.06
92	720 ± 2	78 ± 0	0.82 ± 0.06
93	727 ± 3	76 ± 1	0.83 ± 0.06
94	711 ± 2	74 ± 0	0.78 ± 0.05
95	691 ± 2	74 ± 0	0.81 ± 0.05
96	687 ± 2	68 ± 0	0.89 ± 0.05
97	632 ± 3	29 ± 1	0.73 ± 0.08
98	718 ± 2	77 ± 1	0.71 ± 0.07
99	607 ± 3	74 ± 1	0.84 ± 0.06
100	618 ± 2	63 ± 0	0.71 ± 0.05
101	754 ± 2	72 ± 1	0.80 ± 0.07
106	700 ± 1	85 ± 1	0.80 ± 0.03
107	703 ± 1	76 ± 0	0.85 ± 0.05
108	662 ± 1	84 ± 0	0.77 ± 0.06
110	756 ± 1	121 ± 0	0.42 ± 0.04
112	777 ± 1	114 ± 0	0.48 ± 0.04
114	755 ± 3	89 ± 1	0.98 ± 0.08
115	651 ± 1	83 ± 0	0.76 ± 0.06
116	707 ± 2	83 ± 1	0.84 ± 0.07
117	673 ± 1	86 ± 0	0.75 ± 0.06
118	643 ± 2	80 ± 0	0.95 ± 0.08
121	722 ± 2	69 ± 0	0.85 ± 0.05
122	628 ± 2	75 ± 1	0.73 ± 0.06
123	731 ± 2	79 ± 0	0.70 ± 0.06
124	650 ± 1	81 ± 0	0.84 ± 0.05
127	658 ± 2	81 ± 0	0.74 ± 0.07
128	820 ± 4	70 ± 1	0.80 ± 0.10
129	691 ± 2	92 ± 1	0.86 ± 0.07
131	681 ± 2	82 ± 0	0.75 ± 0.05
132	738 ± 1	73 ± 0	0.74 ± 0.04
133	730 ± 2	74 ± 0	0.72 ± 0.05
134	634 ± 2	84 ± 0	0.88 ± 0.07

135	705 ± 2	71 ± 0	0.85 ± 0.05
136	702 ± 1	68 ± 0	0.89 ± 0.04
137	636 ± 2	72 ± 0	0.83 ± 0.06
139	752 ± 1	71 ± 0	0.79 ± 0.04
140	724 ± 1	73 ± 0	0.79 ± 0.04
141	708 ± 2	82 ± 0	0.82 ± 0.05
142	757 ± 1	76 ± 0	0.74 ± 0.04
143	738 ± 1	77 ± 0	0.84 ± 0.05
144	754 ± 1	91 ± 0	0.77 ± 0.05
146	682 ± 2	82 ± 0	0.72 ± 0.04
147	671 ± 1	86 ± 0	0.88 ± 0.06
148	710 ± 2	77 ± 0	0.78 ± 0.06
149	782 ± 3	78 ± 0	0.72 ± 0.07
150	662 ± 2	86 ± 1	0.75 ± 0.06
152	700 ± 1	82 ± 0	0.91 ± 0.06
154	807 ± 3	79 ± 0	0.69 ± 0.07
155	689 ± 2	80 ± 0	0.94 ± 0.07
156	694 ± 2	87 ± 0	0.78 ± 0.06
157	739 ± 1	79 ± 0	0.80 ± 0.05
158	676 ± 1	74 ± 0	0.79 ± 0.04
159	690 ± 2	74 ± 0	0.86 ± 0.06
160	709 ± 3	78 ± 0	0.75 ± 0.10
161	729 ± 2	78 ± 0	0.83 ± 0.09
162	705 ± 3	73 ± 0	0.77 ± 0.05
164	778 ± 1	73 ± 0	0.79 ± 0.09
165	696 ± 1	75 ± 0	0.77 ± 0.05
166	662 ± 1	82 ± 0	0.87 ± 0.05
167	660 ± 1	86 ± 0	0.82 ± 0.05
169	688 ± 1	97 ± 0	0.65 ± 0.02
170	640 ± 0	178 ± 0	0.42 ± 0.03

Supplementary Table S5: Results from the Lipari and Szabo model-free analysis of the ^{15}N-relaxation data of RhebΔCT bound to GDP with TENSOR2

Residue	Model	χ^2	$S^2 \pm$ error	τ_i [ns] ± error	R_{ex} [s^{-1}] ± error
6	5	0.00(0)	0.94 ± 0.01	0.940 ± 0.451	0.0 ± 0.0
7	5	0.00(0)	0.94 ± 0.01	5.140 ± 3.320	0.0 ± 0.0
8	(6)5	0.17(4)	0.90 ± 0.01	9.900 ± 3.390	0.0 ± 0.0
9	5	0.00(0)	0.87 ± 0.02	3.730 ± 2.920	0.0 ± 0.0
10	(6)5	0.13(8)	0.84 ± 0.02	9.900 ± 3.050	0.0 ± 0.0
11	5	0.00(0)	0.95 ± 0.01	1.460 ± 2.420	0.0 ± 0.0
12	5	0.00(0)	0.97 ± 0.01	1.080 ± 2.560	0.0 ± 0.0
14	1	0.67(7)	0.85 ± 0.00	0.000 ± 0.000	0.0 ± 0.0
15	(6)5	0.51(5)	0.89 ± 0.02	9.900 ± 3.880	0.8 ± 0.0
16	3	0.00(6)	0.84 ± 0.00	0.000 ± 0.000	1.1 ± 0.1
18	5	0.00(0)	0.95 ± 0.01	3.000 ± 3.430	0.0 ± 0.0
19	(6)5	5.68(0)	1.03 ± 0.01	9.900 ± 4.150	0.0 ± 0.0
20	(6)3	3.54(0)	0.82 ± 0.00	0.000 ± 0.000	2.2 ± 0.1
21	(3)3	11.40(0)	0.78 ± 0.00	0.000 ± 0.000	2.3 ± 0.0
22	1	4.59(0)	0.87 ± 0.00	0.000 ± 0.000	0.0 ± 0.0
24	3	1.57(0)	0.85 ± 0.00	0.000 ± 0.000	1.2 ± 0.1
25	(3)3	10.70(0)	0.87 ± 0.00	0.000 ± 0.000	0.2 ± 0.0
26	(6)5	10.50(0)	1.09 ± 0.01	9.900 ± 3.130	0.0 ± 0.0
27	3	1.04(0)	0.84 ± 0.00	0.000 ± 0.000	1.5 ± 0.1
28	3	0.01(8)	0.81 ± 0.00	0.000 ± 0.000	1.5 ± 0.1
29	(6)5	0.69(2)	0.93 ± 0.01	9.840 ± 3.760	0.0 ± 0.0
31	2	0.99(4)	0.78 ± 0.00	0.010 ± 0.004	0.0 ± 0.0
32	2	0.24(5)	0.77 ± 0.00	0.021 ± 0.007	0.0 ± 0.0
33	5	0.00(0)	0.84 ± 0.01	2.330 ± 0.472	0.0 ± 0.0
34	5	0.00(0)	0.81 ± 0.01	3.330 ± 1.350	0.0 ± 0.0
35	5	0.00(0)	0.65 ± 0.00	1.580 ± 0.075	0.0 ± 0.0
36	5	0.00(0)	0.97 ± 0.01	1.720 ± 3.760	0.0 ± 0.0
38	3	0.61(8)	0.83 ± 0.00	0.000 ± 0.000	1.2 ± 0.1
39	2	1.30(0)	0.87 ± 0.00	0.054 ± 0.023	0.0 ± 0.0
40	1	1.69(0)	0.85 ± 0.00	0.000 ± 0.000	0.0 ± 0.0
41	4	0.00(0)	0.73 ± 0.01	0.019 ± 0.006	1.7 ± 0.1
42	3	2.14(0)	0.78 ± 0.00	0.000 ± 0.000	2.6 ± 0.1

43	3	1.94(0)	0.87 ± 0.00	0.000 ± 0.000	1.1 ± 0.1
44	3	0.44(7)	0.79 ± 0.00	0.000 ± 0.000	1.1 ± 0.1
45	3	3.83(0)	0.85 ± 0.00	0.000 ± 0.000	0.8 ± 0.1
46	3	0.01(7)	0.81 ± 0.00	0.000 ± 0.000	1.9 ± 0.1
47	3	1.21(0)	0.84 ± 0.00	0.000 ± 0.000	0.6 ± 0.1
48	3	0.62(1)	0.82 ± 0.00	0.000 ± 0.000	1.6 ± 0.1
51	3	0.03(3)	0.74 ± 0.00	0.000 ± 0.000	2.5 ± 0.1
52	3	1.59(0)	0.76 ± 0.00	0.000 ± 0.000	0.8 ± 0.1
53	4	0.00(0)	0.76 ± 0.01	0.015 ± 0.007	1.7 ± 0.1
54	(6)5	0.83(4)	0.92 ± 0.01	9.900 ± 3.00	0.0 ± 0.0
55	(6)5	0.47(7)	0.94 ± 0.01	9.900 ± 3.500	0.0 ± 0.0
56	5	0.00(0)	0.84 ± 0.03	5.500 ± 2.840	0.0 ± 0.0
57	5	0.00(0)	0.76 ± 0.03	7.530 ± 2.780	0.0 ± 0.0
58	(6)5	2.73(0)	0.48 ± 0.05	9.890 ± 2.100	0.0 ± 0.0
59	(6)5	1.66(0)	0.83 ± 0.02	9.900 ± 3.000	0.0 ± 0.0
60	5	0.00(0)	0.94 ± 0.03	0.794 ± 2.000	0.0 ± 0.0
61	(6)5	4.06(0)	0.85 ± 0.02	9.900 ± 2.940	0.0 ± 0.0
62	4	0.00(0)	0.76 ± 0.01	0.055 ± 0.009	0.8 ± 0.1
63	(6)5	0.73(0)	0.69 ± 0.04	9.890 ± 3.000	0.0 ± 0.0
64	(6)5	4.94(0)	0.92 ± 0.01	9.900 ± 3.420	0.0 ± 0.0
65	3	0.52(9)	0.79 ± 0.00	0.000 ± 0.000	1.0 ± 0.1
66	3	2.49(0)	0.79 ± 0.00	0.000 ± 0.000	0.7 ± 0.1
68	3	0.12(1)	0.80 ± 0.00	0.000 ± 0.000	0.4 ± 0.1
69	6 (4)	1.06(0)	0.20 ± 0.07	9.090 ± 1.740	8.3 ± 0.5
74	3	0.73(6)	0.93 ± 0.00	0.000 ± 0.000	1.2 ± 0.1
75	(6)5	0.08(9)	0.86 ± 0.02	9.900 ± 3.080	0.0 ± 0.0
76	4	0.00(0)	0.77 ± 0.01	0.097 ± 0.012	0.4 ± 0.1
77	3	0.36(5)	0.84 ± 0.00	0.000 ± 0.000	2.7 ± 0.1
78	(6)5	0.04(6)	0.95 ± 0.01	9.840 ± 4.050	0.0 ± 0.0
79	2	3.52(0)	0.83 ± 0.00	0.029 ± 0.008	0.0 ± 0.0
83	5	0.00(0)	0.93 ± 0.01	1.270 ± 1.370	0.0 ± 0.0
84	5	0.00(0)	0.94 ± 0.01	2.560 ± 3.000	0.0 ± 0.0
85	(6)5	5.09(0)	0.98 ± 0.01	9.810 ± 4.000	0.0 ± 0.0

86	3	0.00(5)	0.81 ± 0.00	0.000 ± 0.000	0.3 ± 0.1
87	3	0.18(4)	0.83 ± 0.00	0.000 ± 0.000	2.2 ± 0.1
88	(3)3	8.03(0)	0.84 ± 0.00	0.000 ± 0.000	0.5 ± 0.0
89	3	1.53(0)	0.84 ± 0.00	0.000 ± 0.000	1.3 ± 0.0
90	3	0.81(7)	0.86 ± 0.00	0.000 ± 0.000	0.2 ± 0.1
91	(6)5	21.30(0)	0.97 ± 0.00	9.900 ± 3.790	0.0 ± 0.0
92	3	0.68(1)	0.84 ± 0.00	0.000 ± 0.000	0.7 ± 0.1
93	2	3.29(0)	0.87 ± 0.00	0.037 ± 0.011	0.0 ± 0.0
94	(6)3	5.98(0)	0.81 ± 0.00	0.000 ± 0.000	1.6 ± 0.1
95	3	2.03(0)	0.86 ± 0.00	0.000 ± 0.000	0.8 ± 0.1
96	3	1.96(0)	0.87 ± 0.00	0.000 ± 0.000	2.9 ± 0.1
97	3	0.00(3)	0.87 ± 0.01	0.000 ± 0.000	2.1 ± 0.1
98	3	0.48(4)	0.84 ± 0.00	0.000 ± 0.000	0.3 ± 0.1
99	3	0.32(3)	0.82 ± 0.00	0.000 ± 0.000	0.9 ± 0.1
101	3	0.12(2)	0.86 ± 0.00	0.000 ± 0.000	1.3 ± 0.0
105	3	0.41(4)	0.82 ± 0.00	0.000 ± 0.000	1.1 ± 0.0
106	3	4.00(0)	0.81 ± 0.00	0.000 ± 0.000	0.3 ± 0.0
107	3	0.94(5)	0.82 ± 0.00	0.000 ± 0.000	0.1 ± 0.0
108	5	0.00(0)	0.93 ± 0.01	2.000 ± 0.741	0.0 ± 0.0
109	5	0.00(0)	0.89 ± 0.01	1.280 ± 0.240	0.0 ± 0.0
110	5	0.00(0)	0.71 ± 0.00	1.200 ± 0.062	0.0 ± 0.0
111	5	0.00(0)	0.79 ± 0.01	1.340 ± 0.117	0.0 ± 0.0
112	5	0.00(0)	0.79 ± 0.00	0.899 ± 0.055	0.0± 0.0
115	5	0.00(0)	0.91 ± 0.01	2.130 ± 2.210	0.0 ± 0.0
116	(6)5	6.86(0)	0.90 ± 0.01	9.900 ± 3.280	0.0 ± 0.0
118	(6)5	0.43(7)	0.96 ± 0.01	9.900 ± 3.910	0.0 ± 0.0
119	3	1.32(0)	0.86 ± 0.00	0.000 ± 0.000	0.2 ± 0.1
120	3	2.99(0)	0.76 ± 0.01	0.000 ± 0.000	1.7 ± 0.1
121	3	0.54(5)	0.83 ± 0.00	0.000 ± 0.000	1.5 ± 0.1
122	(6)5	4.11(0)	1.01 ± 0.01	7.680 ± 4.110	0.0 ± 0.0
123	(6)5	5.54(0)	1.01 ± 0.01	3.880 ± 4.480	0.0 ± 0.0
124	2	1.54(0)	0.84 ± 0.00	0.016 ± 0.006	0.0 ± 0.0
125	3	3.19(0)	0.77 ± 0.00	0.000 ± 0.000	1.4 ± 0.1

127	2	2.25(0)	0.85 ± 0.00	0.051 ± 0.013	0.0 ± 0.0
128	3	1.43(0)	0.84 ± 0.00	0.000 ± 0.000	1.3 ± 0.1
129	(6)5	0.12(2)	0.91 ± 0.01	9.900 ± 3.730	0.0 ± 0.0
130	3	1.18(0)	0.82 ± 0.00	0.000 ± 0.000	0.4 ± 0.1
131	(6)5	9.35(0)	0.97 ± 0.00	9.760 ± 3.860	0.0 ± 0.0
132	(6)5	13.40(0)	1.07 ± 0.01	9.900 ± 3.240	0.0 ± 0.0
133	3	0.00(0)	0.82 ± 0.00	0.000 ± 0.000	0.6 ± 0.0
134	5	0.00(0)	0.93 ± 0.01	1.850 ± 2.590	0.0 ± 0.0
135	3	1.56(0)	0.87 ± 0.00	0.000 ± 0.000	0.3 ± 0.1
136	3	2.37(0)	0.86 ± 0.00	0.000 ± 0.000	1.1 ± 0.0
137	5	0.00(0)	0.93 ± 0.01	1.830 ± 3.000	0.0 ± 0.0
138	(6)5	3.74(0)	1.04 ± 0.01	9.900 ± 3.680	0.0 ± 0.0
139	3	2.14(0)	0.84 ± 0.00	0.000 ± 0.000	1.2 ± 0.0
140	3	0.06(1)	0.87 ± 0.00	0.000 ± 0.000	0.8 ± 0.0
141	5	0.00(0)	0.95 ± 0.01	1.720 ± 2.850	0.0 ± 0.0
142	4	0.00(0)	0.73 ± 0.01	0.082 ± 0.012	2.2 ± 0.1
143	(6)3	4.15(0)	0.79 ± 0.00	0.000 ± 0.000	1.6 ± 0.1
144	5	0.00(0)	0.94 ± 0.01	1.300 ± 0.463	0.0 ± 0.0
145	(6)5	4.74(0)	0.96 ± 0.01	9.870 ± 3.660	0.0 ± 0.0
146	(6)5	2.80(0)	0.96 ± 0.01	9.900 ± 3.830	0.0 ± 0.0
147	5	0.00(0)	0.96 ± 0.01	2.540 ± 3.770	0.0 ± 0.0
148	(3)3	11.00(0)	0.85 ± 0.00	0.000 ± 0.000	0.6 ± 0.0
149	3	1.79(0)	0.77 ± 0.00	0.000 ± 0.000	1.5 ± 0.1
150	(6)5	13.20(0)	1.00 ± 0.01	9.900 ± 4.480	0.0 ± 0.0
151	1	2.40(0)	0.86 ± 0.00	0.000 ± 0.000	0.0 ± 0.0
152	5	0.00(0)	0.97 ± 0.01	2.340 ± 3.940	0.0 ± 0.0
154	3	0.73(2)	0.75 ± 0.00	0.000 ± 0.000	1.2 ± 0.1
155	(6)5	0.06(4)	0.87 ± 0.02	9.900 ± 3.450	0.0 ± 0.0
156	(6)5	1.17(0)	0.92 ± 0.01	9.900 ± 3.700	0.0 ± 0.0
157	3	3.25(0)	0.84 ± 0.00	0.000 ± 0.000	0.9 ± 0.1
158	3	1.32(0)	0.87 ± 0.00	0.000 ± 0.000	0.6 ± 0.1
159	3	0.49(6)	0.87 ± 0.01	0.000 ± 0.000	0.5 ± 0.1
160	3	0.11(1)	0.86 ± 0.00	0.000 ± 0.000	0.5 ± 0.1

161	3	0.71(5)	0.83 ± 0.01	0.000 ± 0.000	0.9 ± 0.1
163	4	0.00(0)	0.88 ± 0.01	0.059 ± 0.016	0.2 ± 0.1
164	3	0.13(6)	0.83 ± 0.00	0.000 ± 0.000	1.2 ± 0.1
165	4	0.00(0)	0.87 ± 0.01	0.044 ± 0.013	0.4 ± 0.1
166	3	0.19(9)	0.86 ± 0.00	0.000 ± 0.000	0.5 ± 0.0
167	(6)5	0.27(5)	0.89 ± 0.01	9.900 ± 3.000	0.0 ± 0.0
168	5	0.00(0)	0.90 ± 0.01	1.200 ± 0.175	0.0 ± 0.0
169	5	0.00(0)	0.69 ± 0.01	1.540 ± 0.102	0.0 ± 0.0
170	5	0.00(0)	0.39 ± 0.00	1.810 ± 0.085	0.0 ± 0.0

Supplementary Table S6: Results from the Lipari and Szabo model-free analysis of the ^{15}N-relaxation data of RhebΔCT bound to GppNHp with TENSOR2

Residue	Model	χ^2	S^2 ± error	τ_i [ns] ± error	R_{ex} [s^{-1}] ± error
4	5	0.00(0)	0.59 ± 0.01	0.95 ± 0.07	0.0 ± 0.0
5	5	0.00(0)	0.74 ± 0.01	1.00 ± 0.12	0.0 ± 0.0
6	2	4.46(0)	0.75 ± 0.00	0.03 ± 0.00	0.0 ± 0.0
7	(6)5	1.61(0)	0.88 ± 0.02	10.40 ± 3.67	0.0 ± 0.0
8	(6)5	0.06(5)	0.86 ± 0.02	10.40 ± 3.62	0.0 ± 0.0
9	5	0.00(0)	0.92 ± 0.01	1.82 ± 2.57	0.0 ± 0.0
10	5	0.00(0)	0.90± 0.01	1.36 ± 2.64	0.0 ± 0.0
11	5	0.00(0)	0.94 ± 0.01	2.33 ± 3.66	0.0 ± 0.0
12	(6)5	0.57(5)	0.96 ± 0.01	10.40 ± 4.23	0.0 ± 0.0
13	5	0.00(0)	0.87 ± 0.02	5.90 ± 3.56	0.0 ± 0.0
14	(6)5	0.85(0)	0.97 ± 0.01	10.40 ± 4.54	0.0 ± 0.0
16	(6)5	1.35(0)	0.79 ± 0.03	10.40 ± 3.38	0.0 ± 0.0
17	5	0.00(0)	0.94 ± 0.01	2.86 ± 4.10	0.0 ± 0.0
18	3	0.03(0)	0.71 ± 0.00	0.00 ± 0.00	1.9 ± 0.1
20	3	0.15(7)	0.83 ± 0.00	0.00 ± 0.00	2.9 ± 0.1
21	3	0.37(2)	0.81 ± 0.00	0.00 ± 0.00	0.3 ± 0.1
22	3	0.00(0)	0.83 ± 0.00	0.00 ± 0.00	1.3 ± 0.0
23	3	1.37(0)	0.75 ± 0.01	0.00 ± 0.00	0.5 ± 0.2
26	3	0.12(4)	0.85 ± 0.00	0.00 ± 0.00	1.4 ± 0.1

27	3	0.15(2)	0.81 ± 0.00	0.00 ± 0.00	2.2 ± 0.1
28	5	0.00(0)	0.94 ± 0.01	4.00 ± 0.00	0.0 ± 0.0
29	(6)5	2.62(0)	0.91 ± 0.01	10.40 ± 3.84	0.0 ± 0.0
43	3	0.01(2)	0.85 ± 0.00	0.00 ± 0.00	0.9 ± 0.1
44	(6)5	7.07(0)	0.92 ± 0.01	10.40 ± 3.90	0.0 ± 0.0
45	5	0.00(0)	0.97 ± 0.01	1.86 ± 3.84	0.0± 0.0
46	5	0.00(0)	0.91 ± 0.02	2.93 ± 3.51	0.0 ± 0.0
47	3	2.14(0)	0.84 ± 0.00	0.00 ± 0.00	0.2 ± 0.0
48	(6)5	0.05(4)	0.97 ± 0.00	10.40 ± 4.14	0.0 ± 0.0
49	5	0.00(0)	0.93 ± 0.01	2.08 ± 2.81	0.0 ± 0.0
51	4	0.00(0)	0.70 ± 0.01	0.02 ± 0.01	0.3 ± 0.1
52	3	4.46(0)	0.74 ± 0.00	0.00 ± 0.00	1.7 ± 0.0
53	2	0.13(5)	0.76 ± 0.00	0.01 ± 0.00	0.0± 0.0
54	4	0.00(0)	0.76 ± 0.01	0.03 ± 0.00	0.7 ± 0.1
55	5	0.00(0)	0.98 ± 0.01	1.61 ± 0.00	0.0 ± 0.0
56	5	0.00(0)	0.93 ± 0.01	1.25 ± 0.00	0.0 ± 0.0
57	5	0.00(0)	0.96 ± 0.01	0.91 ± 3.00	0.0± 0.0
58	(6)5	1.20(0)	0.89 ± 0.01	10.40 ± 3.89	0.0 ± 0.0
59	(6)5	1.94(0)	0.88 ± 0.02	10.40 ± 3.76	0.0 ± 0.0
63	3	1.37(0)	0.72 ± 0.00	0.00 ± 0.00	2.0 ± 0.1
65	4	0.00(0)	0.75 ± 0.01	0.02 ± 0.01	0.4 ± 0.1
66	3	0.28(4)	0.81 ± 0.01	0.00 ± 0.00	0.9 ± 0.2
67	1	4.42(0)	0.87 ± 0.00	0.00 ± 0.00	0.0 ± 0.0
68	3	0.08(0)	0.76 ± 0.00	0.00 ± 0.00	0.7 ± 0.0
77	5	0.00(0)	0.95 ± 0.01	2.11 ± 4.14	0.0 ± 0.0
79	5	0.00(0)	0.92 ± 0.01	1.00 ± 0.64	0.0 ± 0.0
80	5	0.00(0)	0.83 ± 0.01	1.77 ± 0.63	0.0 ± 0.0
81	3	1.74(0)	0.86 ± 0.00	0.00 ± 0.00	0.2 ± 0.1
82	5	0.00(0)	0.94 ± 0.01	2.48 ± 3.63	0.0 ± 0.0
83	(6)5	0.58(6)	0.84 ± 0.02	10.40 ± 3.63	0.0 ± 0.0
84	(6)5	3.59(0)	0.93 ± 0.01	10.40 ± 4.14	0.0 ± 0.0
85	(6)5	1.79(0)	0.99 ± 0.01	10.40 ± 4.67	0.0± 0.0
86	1	6.31(0)	0.85 ± 0.00	17 ± 0.00	0.0 ± 0.0

87	(6)3	3.49(0)	0.84 ± 0.00	0.00 ± 0.00	3.2 ± 0.1
88	3	0.42(3)	0.82 ± 0.00	0.00 ± 0.00	0.9 ± 0.0
90	5	0.00(0)	0.98 ± 0.01	2.17 ± 4.56	0.0 ± 0.0
92	(6)5	1.13(0)	0.96 ± 0.01	10.40 ± 4.17	0.0 ± 0.0
93	3	1.22(0)	0.83 ± 0.00	0.00 ± 0.00	0.2 ± 0.0
94	3	1.47(0)	0.85 ± 0.00	0.00 ± 0.00	0.8 ± 0.0
95	3	0.00(1)	0.84 ± 0.00	0.00 ± 0.00	0.9 ± 0.0
96	3	0.70(5)	0.83 ± 0.00	0.00 ± 0.00	2.2 ± 0.0
97	3	0.45(5)	0.88 ± 0.00	0.00 ± 0.00	0.2 ± 0.1
98	5	0.00(0)	1.07 ± 0.01	1.09 ± 1.78	0.0 ± 0.0
99	3	0.01(5)	0.83 ± 0.00	0.00 ± 0.00	1.7 ± 0.0
100	3	0.70(2)	0.76 ± 0.00	0.00 ± 0.00	3.4± 0.0
101	(3)3	10.60(0)	0.86 ± 0.00	0.00 ± 0.00	0.5 ± 0.0
102	3	1.37(0)	0.81 ± 0.00	0.00 ± 0.00	1.2 ± 0.0
107	4	0.00(0)	0.77 ± 0.01	0.03 ± 0.01	1.8 ± 0.1
108	5	0.00(0)	0.89 ± 0.01	1.23 ± 0.26	0.0 ± 0.0
109	3	0.67(1)	0.76 ± 0.00	0.00 ± 0.00	0.2 ± 0.1
110	5	0.00(0)	0.75 ± 0.01	1.11 ± 0.07	0.0 ± 0.0
111	5	0.00(0)	0.75 ± 0.01	1.47 ± 0.17	0.0 ± 0.0
112	5	0.00(0)	0.77 ± 0.01	0.92 ± 0.06	0.0 ± 0.0
114	5	0.00(0)	0.92 ± 0.01	1.71 ± 3.21	0.0 ± 0.0
115	5	0.00(0)	0.93 ± 0.01	1.66 ± 2.44	0.0 ± 0.0
116	5	0.00(0)	0.86 ± 0.02	2.80 ± 2.78	0.0 ± 0.0
117	(6)5	0.20(0)	0.86 ± 0.02	10.40 ± 3.56	0.0 ± 0.0
118	(6)3	7.98(0)	0.81 ± 0.00	0.00 ± 0.00	0.7 ± 0.1
119	(6)5	0.29(5)	0.98 ± 0.00	10.40 ± 4.25	0.0 ± 0.0
120	3	0.01(3)	0.81 ± 0.00	0.00 ± 0.00	0.0 ± 0.5
121	(6)3	5.65(0)	0.82 ± 0.00	0.00 ± 0.00	1.9± 0.0
122	(6)5	3.12(0)	1.02 ± 0.04	0.19 ± 3.84	0.0 ± 0.0
123	(3)3	8.72(0)	0.84 ± 0.00	0.00 ± 0.00	0.3 ± 0.0
124	3	0.00(9)	0.80 ± 0.00	0.00 ± 0.00	0.4 ± 0.0
126	4	0.00(0)	0.77 ± 0.01	0.03 ± 0.01	0.8 ± 0.1
127	(6)5	0.28(0)	0.98± 0.00	10.30 ± 4.17	0.0 ± 0.0

128	3	0.61(6)	0.87 ± 0.00	0.00 ± 0.00	1.9 ± 0.1
129	5	0.00(0)	0.91 ± 0.01	1.91 ± 3.32	0.0 ± 0.0
130	3	0.25(2)	0.80 ± 0.00	0.00 ± 0.00	0.1 ± 0.0
131	1	4.94(0)	0.82 ± 0.00	0.00 ± 0.00	0.0 ± 0.0
132	3	2.69(0)	0.80 ± 0.00	0.00 ± 0.00	0.8 ± 0.0
133	3	0.05(3)	0.82 ± 0.00	0.00 ± 0.00	1.1 ± 0.0
134	(6)5	1.34(0)	0.89 ± 0.02	10.40 ± 3.62	0.0 ± 0.0
135	3	0.81(1)	0.84 ± 0.00	0.00 ± 0.00	1.3± 0.0
136	3	1.36(0)	0.82 ± 0.00	0.00 ± 0.00	1.5 ± 0.0
137	3	0.00(2)	0.87 ± 0.00	0.00 ± 0.00	1.0 ± 0.0
138	3	2.73(0)	0.84 ± 0.00	0.00 ± 0.00	0.6 ± 0.0
139	3	0.66(0)	0.83 ± 0.00	0.00 ± 0.00	1.3 ± 0.0
140	3	0.03(5)	0.79 ± 0.00	0.00 ± 0.00	1.7 ± 0.0
141	1	1.89(0)	0.81 ± 0.00	0.00 ± 0.00	0.0 ± 0.0
142	3	0.01(6)	0.79 ± 0.00	0.00 ± 0.00	1.9 ± 0.0
143	3	1.06(0)	0.80 ± 0.00	0.00 ± 0.00	1.5 ± 0.0
144	5	0.00(0)	0.92 ± 0.01	1.39 ± 0.67	0.0 ± 0.0
145	(6)5	6.19(0)	0.98 ± 0.00	10.40 ± 4.23	0.0 ± 0.0
146	3	0.19(4)	0.84 ± 0.00	0.00 ± 0.00	0.1 ± 0.0
147	5	0.00(0)	0.98 ± 0.01	1.06 ± 3.25	0.0± 0.0
148	3	0.03(5)	0.85 ± 0.00	0.00± 0.00	0.7 ± 0.0
149	3	0.49(7)	0.76 ± 0.00	0.00 ± 0.00	1.1 ± 0.1
150	(6)5	4.01(0)	0.98 ± 0.01	10.40 ± 4.53	0.0 ± 0.0
151	3	0.09(7)	0.83 ± 0.00	0.00 ± 0.00	0.3 ± 0.0
152	3	0.03(7)	0.82 ± 0.00	0.00 ± 0.00	0.5 ± 0.0
154	3	1.05(0)	0.81 ± 0.00	0.00 ± 0.00	0.5 ± 0.1
155	3	0.96(6)	0.85 ± 0.00	0.00 ± 0.00	0.5 ± 0.0
156	5	0.00(0)	0.96 ± 0.01	2.00 ± 3.44	0.0 ± 0.0
157	3	0.00(2)	0.82 ± 0.00	0.00 ± 0.00	0.9 ± 0.0
158	3	2.50(0)	0.83 ± 0.00	0.00 ± 0.00	1.3 ± 0.0
159	3	1.12(0)	0.85 ± 0.00	0.00 ± 0.00	0.9 ± 0.0
160	(6)5	1.38(0)	0.94 ± 0.01	10.40 ± 4.26	0.0 ± 0.0
162	3	0.02(4)	0.86 ± 0.00	0.00 ± 0.00	1.2 ± 0.0

164	3	0.14(7)	0.84 ± 0.00	0.00 ± 0.00	0.6 ± 0.0
165	3	1.78(0)	0.86 ± 0.00	0.00 ± 0.00	0.8 ± 0.0
166	3	0.13(9)	0.85 ± 0.00	0.00 ± 0.00	0.1 ± 0.0
167	(6)5	0.31(4)	0.99 ± 0.00	10.40 ± 4.54	0.0 ± 0.8
168	2	1.28(0)	0.81 ± 0.00	0.02 ± 0.00	0.0 ± 0.0
169	5	0.00(0)	0.84 ± 0.00	1.23 ± 0.06	0.0 ± 0.0
170	5	0.00(0)	0.42 ± 0.00	1.77 ± 0.06	0.0 ± 0.0

Supplementary Figure Legends

Fig. S1: ^{1}H-^{15}(1,2) spectrum of RhebΔCT in the GDP-bound state. The assignments are indicated by the one letter amino acid code and the sequence position. Side chain amide proton resonances of glutamine and asparagine residues are connected by black lines. The resonances of some residues (assignment labels in brackets) are only visible at lower contour level. Negative peaks (red) correspond to residues that are spectrally folded.

Fig. S2: ^{1}H-^{15}N HSQC spectrum of RhebΔCT in the GppNHp-bound state. The assignments are indicated by the one letter amino acid code and the sequence position. Side chain amide proton resonances of glutamine and asparagine residues are connected by black lines. The resonances of some residues (assignment labels in brackets) are only visible at lower contour level. Negative peaks (red) correspond to residues that are spectrally folded.

Fig. S3: (A) Superposition of the ^{1}H-^{15}N HSQC spectra of RhebΔCT in the GppNHp- (red) and GppCp- (green) bound states. **(B)** Larger ^{1}H-^{15}N HSQC spectrum of RhebΔCT in the GppCp-bound state. The assignments are indicated by the one letter amino acid code and the sequence position. Side chain amide proton resonances of glutamine and asparagine residues are connected by black lines. The resonances of some residues (assignment labels in brackets) are only visible at lower contour level. Negative peaks (red) correspond to residues that are spectrally folded.

Fig. S4: Comparison of the backbone dynamics of RhebΔCT in the GppNHp- (red) and GppCp- (green) bound states. Shown are plots of the ^{15}N-relaxation data including ^{15}N-T_1 (top panel), -T_2 (second panel), and {^{1}H}-^{15}N NOE (third panel) values. The location of the

G-boxes and the switch 1 and 2 (SW1 & 2) regions (1,2) and the secondary structure elements are indicated at the top. Filled grey arrows represent β-sheet conformation and grey spirals helical conformation. The secondary structure content was derived from the solution structure of rat Rheb-GDP (PDB-ID 2L0X) (3). That of mouse Rheb-GppNHp is almost identical (PDB- ID 4O25) (4). A superposition of the respective ^{1}H-^{15}N HSQC spectra is shown in SI Fig. S3A.

Fig. S5: More NMR data recorded to characterize the interaction between RhebΔCT and FKBP38-BD. **(A)** View of the structure of mouse Rheb-GppNHp with the spectral changes observed in Fig. 3D mapped onto it (magenta – weak to medium and orange – very weak chemical shift changes. The representation corresponds to a view from the top (= 90° rotation around a horizontal axis) on the structure a shown in Fig. 3E (left side). **(B)** Superposition of the ^{1}H-^{15}N HSQC spectra of ^{15}N-RhebΔCT-GppNHp in the presence of increasing concentrations of unlabeled FKBP38-BD. The color coding and the molar ratios of the two proteins are indicated in the upper left. The residues that showed medium (magenta) or weak (orange) shifts comparing ^{15}N-RhebΔCT-GppNHp in the absence (black) and presence of unlabeled FKBP38-BD (red) in Fig. 3C are labeled in the same color coding. The boxed region contains peaks for the side chain -NH_2 groups of glutamines and asparagines. **(C-E)** Superposition of the ^{1}H-^{15}N HSQC spectra of ^{15}N- FKBP38-BD in the presence of increasing concentrations of unlabeled RhebΔCT-GDP or –GppNHp or a 13mer peptide corresponding to the switch 1 region of Rheb, respectively. The color coding and the molar ratios of the two components are indicated in the upper left. **(F)** Superposition of the ^{1}H-^{15}N HSQC spectra of ^{15}N-RhebΔCT-GppCp in the absence (black) and presence of unlabeled FKBP38-BD (red). That ^{15}N-RhebΔCT-GppCp did not show the same shifts as the GppNHp state may be explained by the fact that it was not fully exchanged, which is indicated by a few remaining peaks of the GDP state (most black peaks with no red peaks on top). Since the latter disappeared upon addition of FKBP38-BD, its presence appeared to have stimulated the further exchange from the GDP to the GppCp state of RhebΔCT. Note that the exchange of GDP to the GTP-analogue GppNHp occurred generally faster during the sample preparation for the NMR studies (see methods) than to GppCp using otherwise the same conditions.

Fig. S6: NMR data recorded to characterize a potential influence of the addition of $CaCl_2$ on the interaction between FKBP38-BD and RhebΔCT. **(A)** Superposition of the ^{1}H-^{15}N HSQC spectra of ^{15}N- FKBP38-BD in the absence (black) and presence of 2 mM $CaCl_2$ (red) in the buffer. Two of the residues of FKBP38-BD that have been suggested to weakly interact with Ca^{2+} (5) are labeled with the one letter amino acid code and the sequence position in the full-length protein and in brackets in the protein used in the published study (5). **(B)** Superposition of the ^{1}H-^{15}N HSQC spectra of ^{15}N- FKBP38-BD in the presence of only 2 mM $CaCl_2$ in the buffer in the absence (black) and presence of unlabeled RhebΔCT-GppNHp (red). **(C)** Superposition of the ^{1}H-^{15}N HSQC spectra of ^{15}N-RhebΔCT-GppNHp in the absence (black) and presence of unlabeled FKBP38-BD and 2 mM $CaCl_2$ (red). The residues that showed medium (magenta) or weak (orange) shifts comparing ^{15}N-RhebΔCT-GppNHp in the absence (black) and presence of unlabeled FKBP38-BD (red) in Fig. 3C are labeled in the same color coding. The boxed region contains peaks for the side chain -NH_2 groups of glutamines and asparagines. Most of the medium shifting ones such as G101, H100, K97 or I99 show also shifts here. However R7 and I47 did not show significant shifts. The peak of the side chain amide proton of W141 has presumably a slightly different peak position as in Fig. 3C and overlaps here with L12. Most of the residues showing weak shifts in the Fig. 3C (orange labels) do not show a significant shift here. Presumably because of the slightly different buffer conditions (+/- 2 mM $CaCl_2$) and slight differences in the used protein concentrations and corresponding molar ratios.

Fig. S7: Comparison of the backbone dynamics of RhebΔCT in the GppNHp-bound state in the absence (red) and presence (blue) of unlabeled FKBP38-BD. Shown are plots of the ^{15}N relaxation data including ^{15}N-T_1 (top panel), -T_2 (second panel), and {^{1}H}-^{15}N NOE (third panel) values. The location of the G-boxes and the switch 1 and 2 (SW1 & 2) regions and the secondary structure elements are indicated at the top. Filled grey arrows represent β-sheet conformation and grey spirals helical conformation. The secondary structure content was derived from the solution structure of rat Rheb-GDP (PDB-ID 2L0X) (3). That of mouse Rheb-GppNHp is almost identical (PDB- ID 4O25) (4). A superposition of the respective ^{1}H-^{15}N HSQC spectra is shown in Fig. 3C.

Fig. S8: More NMR data regarding the effect of FKBP38-BD on the GDP to GppNHp exchange of RhebΔCT. (A-F) Superpositions of the ^{1}H-^{15}N HSQC spectra of ^{15}N-RhebΔCT-GDP in the presence of GppNHp and if indicated at the top of unlabeled FKBP38-BD at a molar rate of 1:102 and/or catalytic amounts of Antarctic phosphatase (= PPase) after different incubation times. The color coding is indicated in upper left of each plot. The ^{1}H-^{15}N crosspeaks of the residues of RhebΔCT-GDP showing strong chemical shift changes to the GppNHp-bound state and that have been considered for the rate analysis are labeled with the one letter amino acid code and the sequence position. The corresponding analysis for the shown series **A** and **B** (**A1/B1** - only FKBP38-BD present, **A2/B2** - FKBP38-BD and PPase present, **A3/B3** only PPase present) are displayed as a function of the residue sequence position in SI Fig. S10 (C) and (D), respectively.

Fig. S9: More NMR data regarding the effect of FKBP38-BD on the GDP to GppNHp exchange of RhebΔCT. (A-E) Superpositions of the ^{1}H-^{15}N HSQC spectra of ^{15}N-RhebΔCT-GDP in the presence of GppNHp and if indicated at the top of unlabeled FKBP38-BD at a molar rate of 1:102 (series **C**) or 1:96 (series **F**) and or catalytic amounts of Antarctic phosphatase (= PPase) after different incubation times. The color coding is indicated in the upper left of each plot. The ^{1}H-^{15}N crosspeaks of the residues of RhebΔCT-GDP showing strong chemical shift changes to the GppNHp-bound state and that have been considered for the rate analysis are labeled with the one letter amino acid code and the residue number. The corresponding analysis for the shown series **C** and **F** (**C1/F1**, only FKBP38-BD present, **C2/F2** - FKBP38-BD and PPase present, **C3/F3** only PPase present) are displayed as a function of the residue sequence position in SI Fig. S10 (E) and (F), respectively.

Fig. S10: Superposition of the ^{1}H-^{15}N HSQC spectra of ^{15}N-RhebΔCT-GDP in the presence of GppNHp and unlabeled FKBP38-BD at a molar rate of 1:15 (series **H**) and either catalytic amounts of Antarctic phosphatase (= PPase) (A) or no Antarctic phosphatase (B) after different incubation times. The color coding is indicated in the upper left of each plot. If FKBP38-BD is present in such high concentrations compared to Rheb the exchange is so fast that the peaks of the starting GDP state are mostly not visible anymore. Thus the peaks of the target GppNHp and not of the starting GDP state have been labeled with the one letter amino acid code and the sequence position. **(C-F)** Plots of the determined exchange times τ_{ex} as a function of the residue sequence position for the series A-C and F (see also Fig. 4A-B, SI Fig. S8-S9, and table 1).

Fig. S11: Picture of the alignment of the amino acid sequences of human Rheb, Ras (p21ras), and Cdc42. The respective Uniprot codes are given at the beginning of each line. The figure was made using MultAlin (6) for the alignment and ESPript (7) for the illustration of the alignment.

Supplementary References

1. Wittinghofer, A., and Vetter, I. R. (2011) Structure-function relationships of the G domain, a canonical switch motif. *Annu Rev Biochem* **80**, 943-971
2. Heard, J. J., Fong, V., Bathaie, S. Z., and Tamanoi, F. (2014) Recent progress in the study of the Rheb family GTPases. *Cellular signalling* **26**, 1950-1957
3. Karassek, S., Berghaus, C., Schwarten, M., Goemans, C. G., Ohse, N., Kock, G., Jockers, K., Neumann, S., Gottfried, S., Herrmann, C., Heumann, R., and Stoll, R. (2010) Ras homolog enriched in brain (Rheb) enhances apoptotic signaling. *The Journal of biological chemistry* **285**, 33979-33991
4. Mazhab-Jafari, M. T., Marshall, C. B., Ho, J., Ishiyama, N., Stambolic, V., and Ikura, M. (2014) Structure-guided mutation of the conserved G3-box glycine in Rheb generates a constitutively activated regulator of mammalian target of rapamycin (mTOR). *The Journal of biological chemistry* **289**, 12195-12201
5. Maestre-Martinez, M., Haupt, K., Edlich, F., Neumann, P., Parthier, C., Stubbs, M. T., Fischer, G., and Lucke, C. (2011) A charge-sensitive loop in the FKBP38 catalytic domain modulates Bcl-2 binding. *Journal of molecular recognition : JMR* **24**, 23-34
6. Corpet, F. (1988) Multiple sequence alignment with hierarchical clustering. *Nucleic acids research* **16**, 10881-10890
7. Robert, X., and Gouet, P. (2014) Deciphering key features in protein structures with the new ENDscript server. *Nucleic acids research* **42**, W320-324

De Cicco et al.
SI Fig. S1

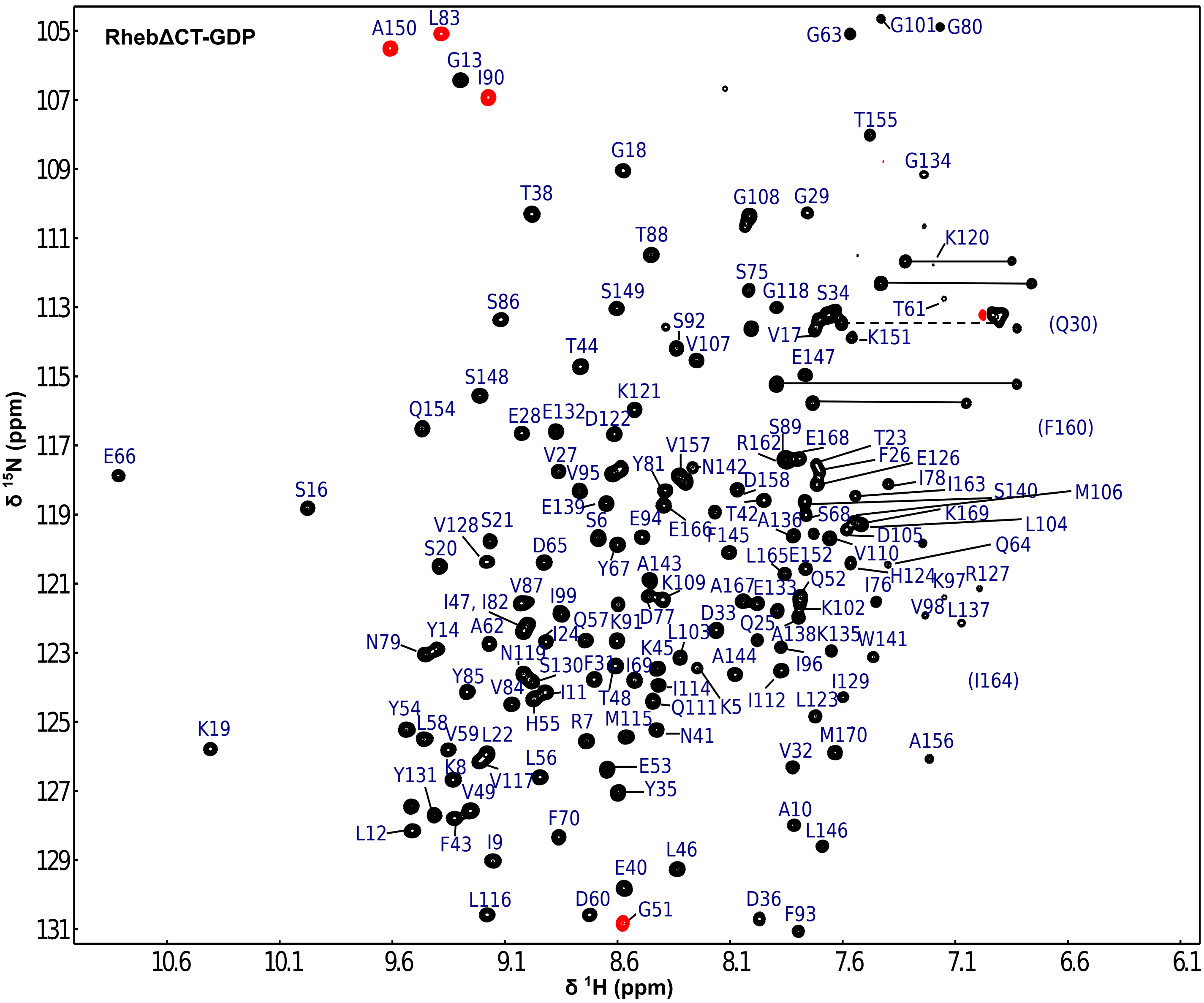

De Cicco et al.
SI Fig. S2

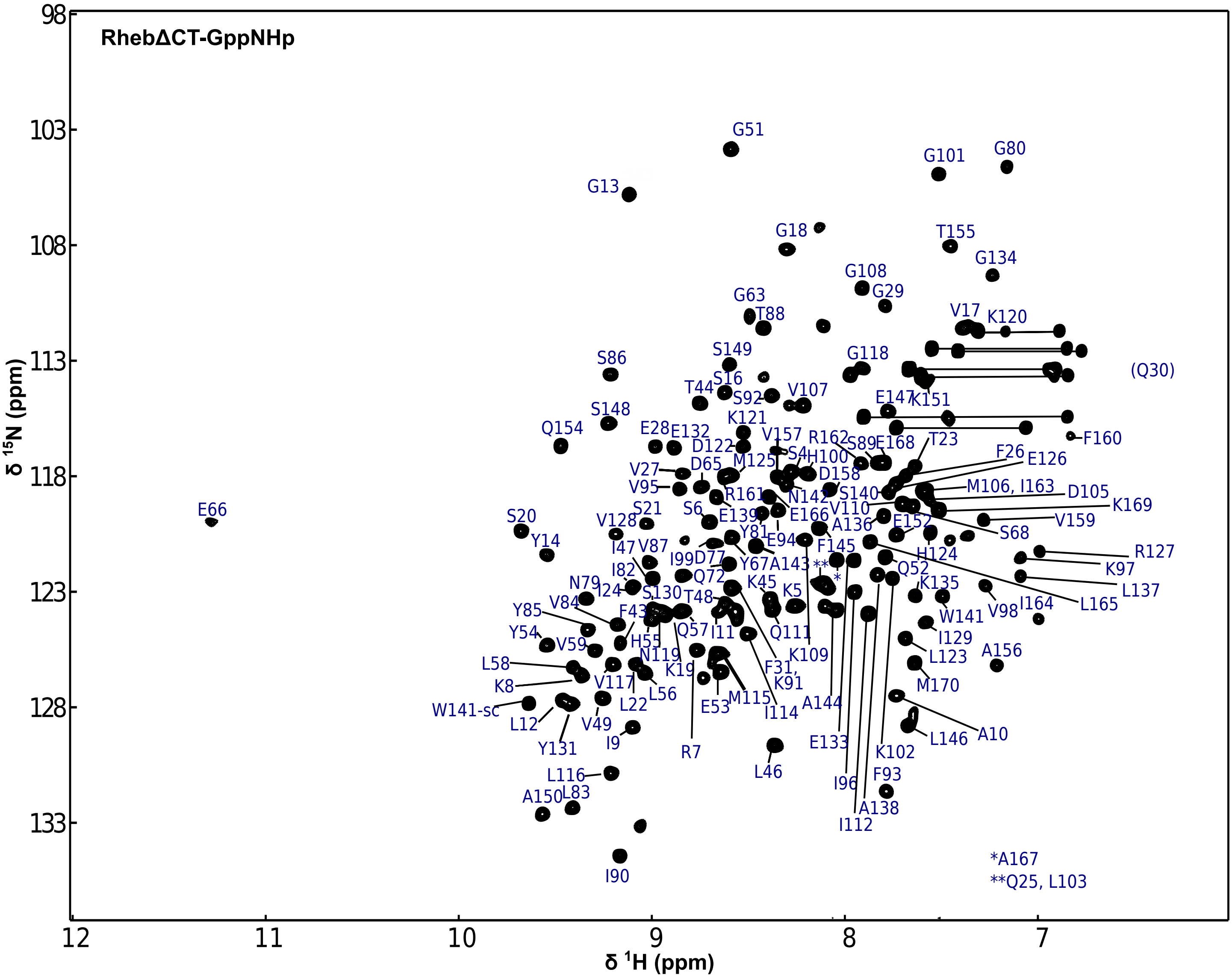

De Cicco et al.
SI Fig. S3

A

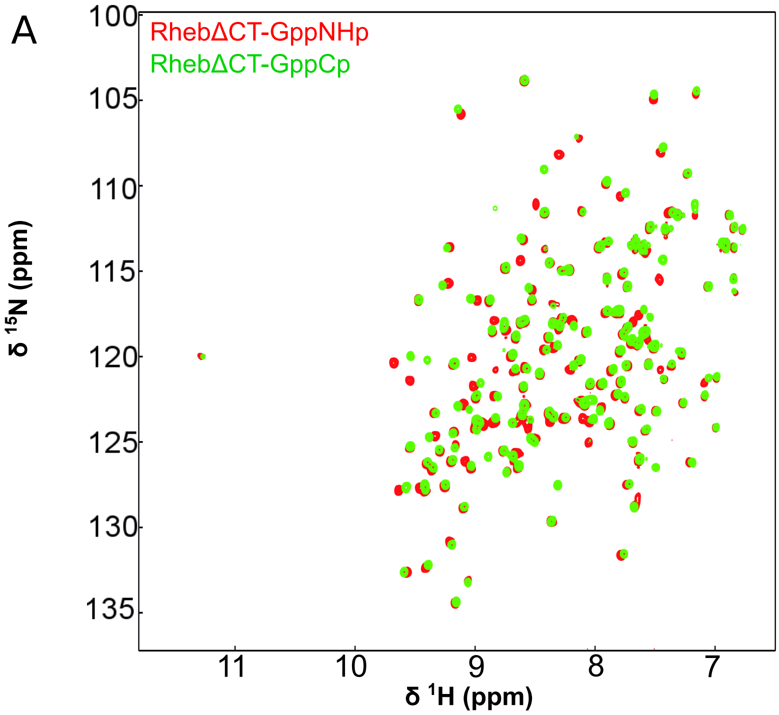

B

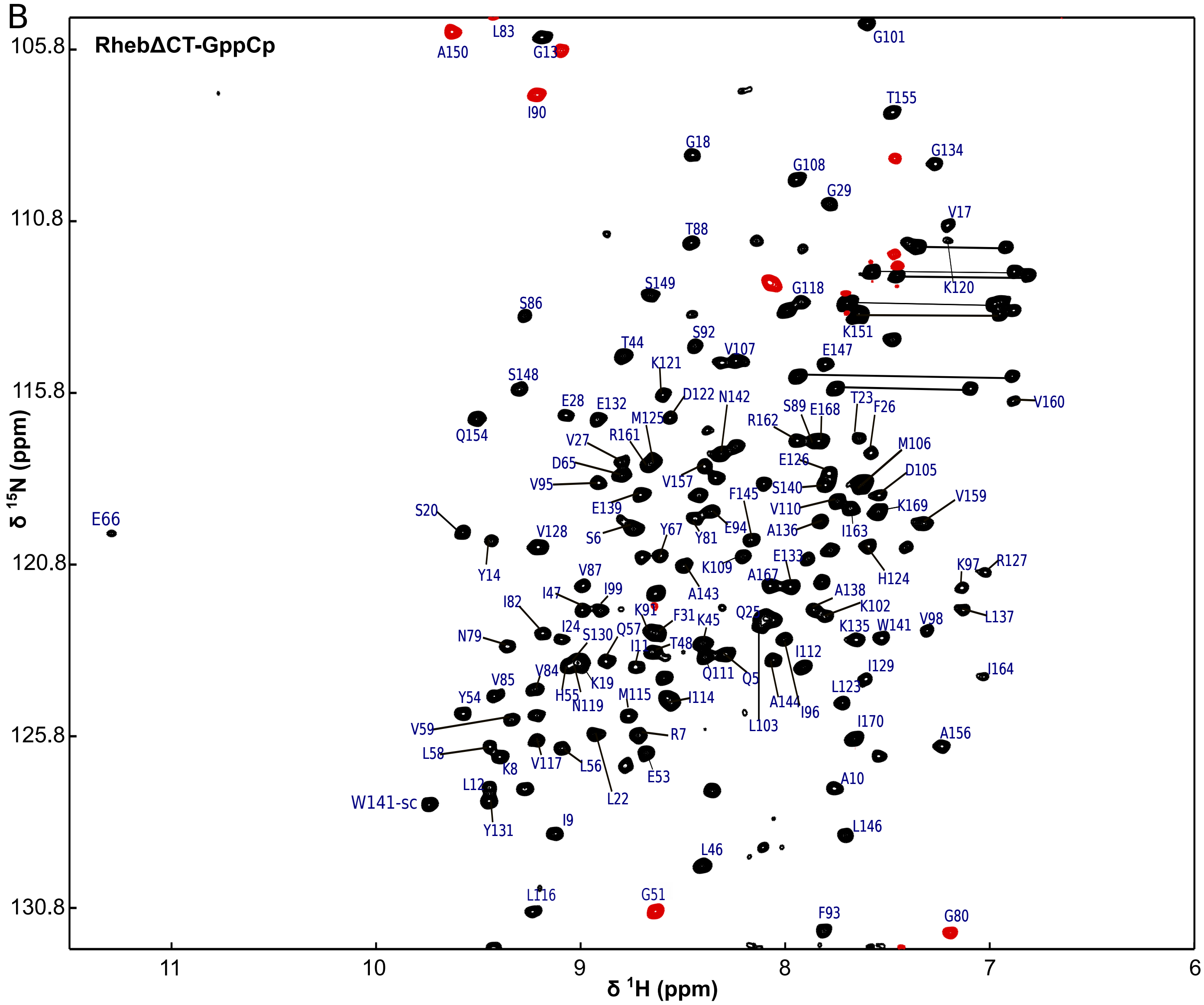

De Cicco et al.
SI Fig. S4

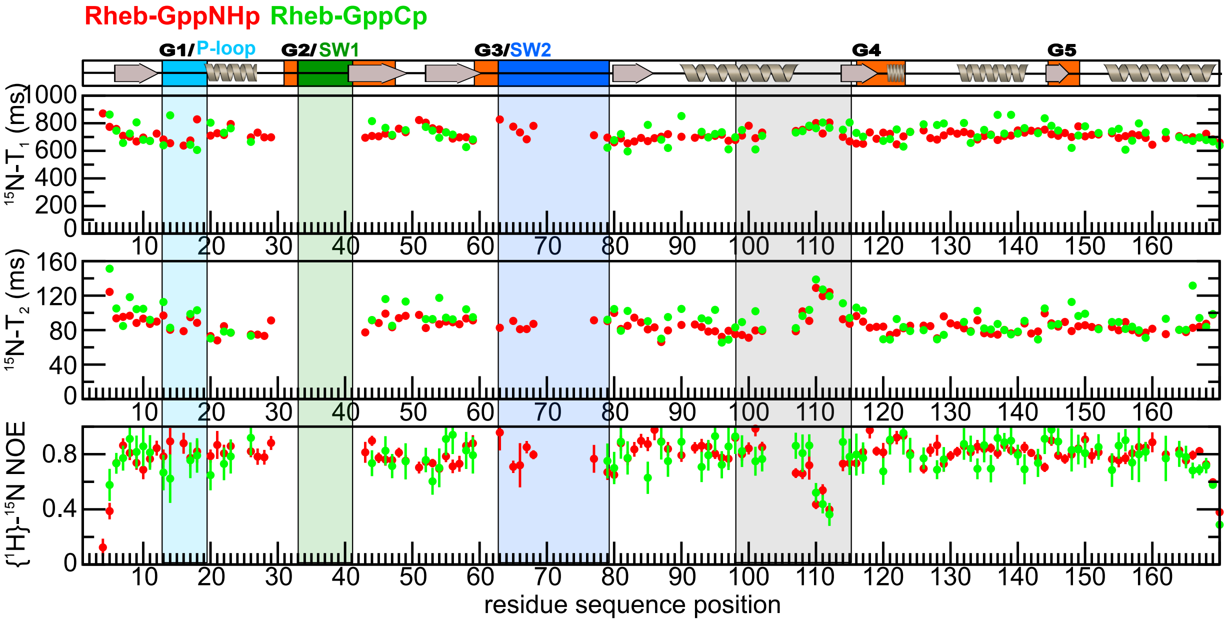

De Cicco et al.
SI Fig. S5

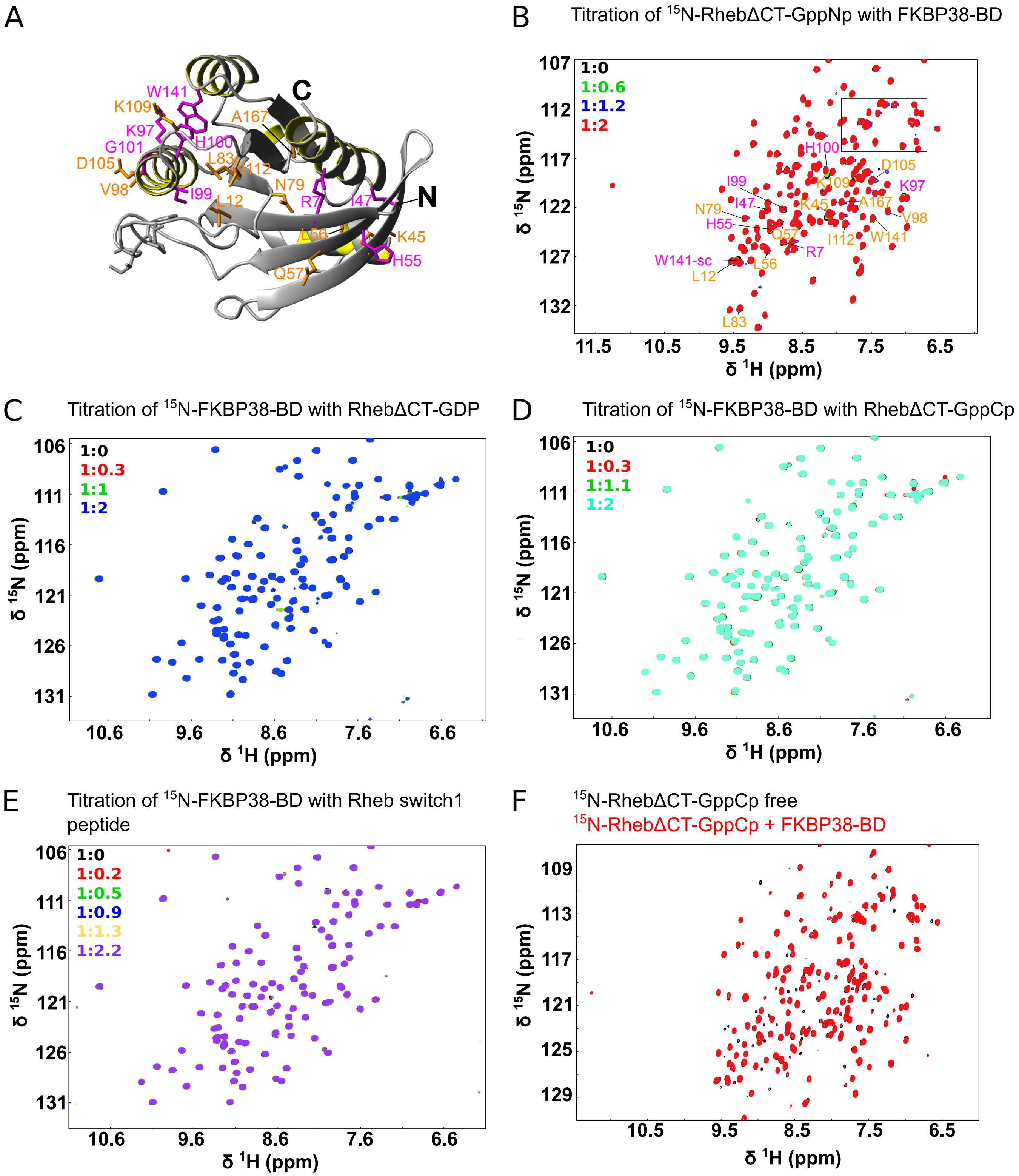

De Cicco et al.
SI Fig. S6

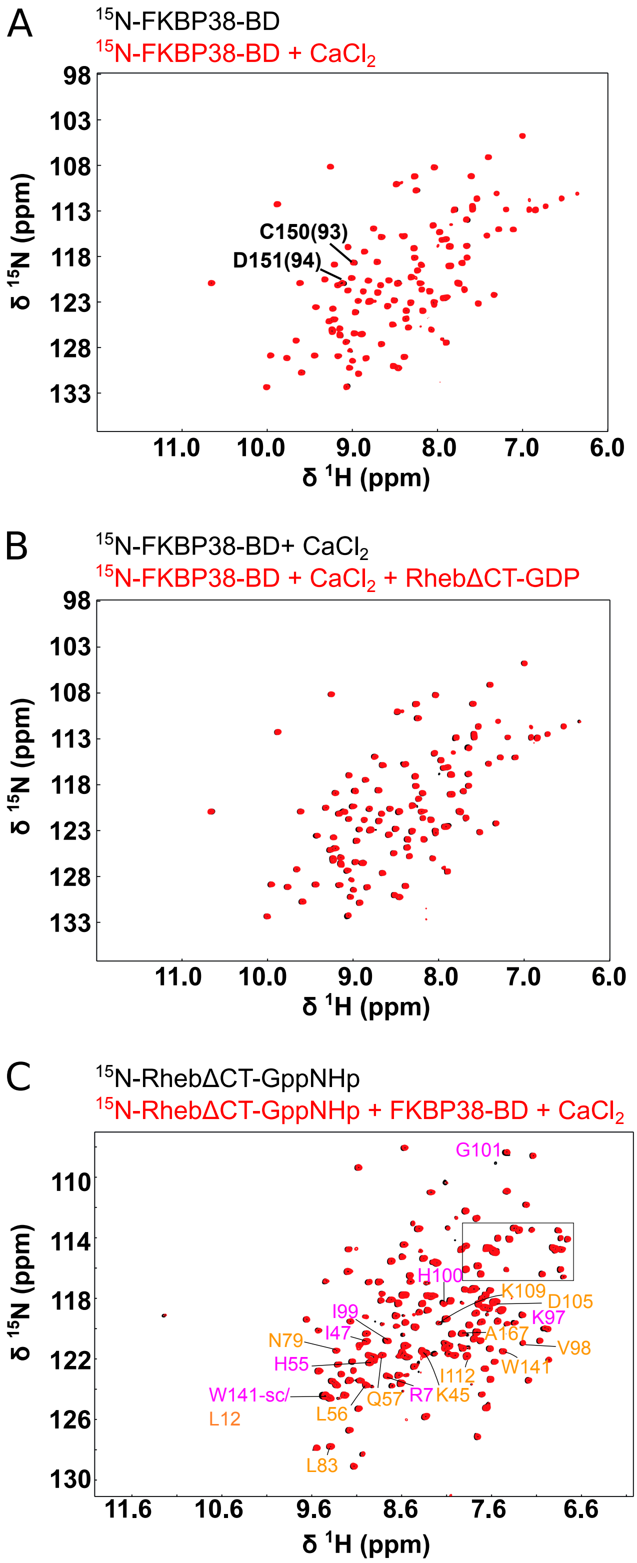

De Cicco et al.
SI Fig. S7

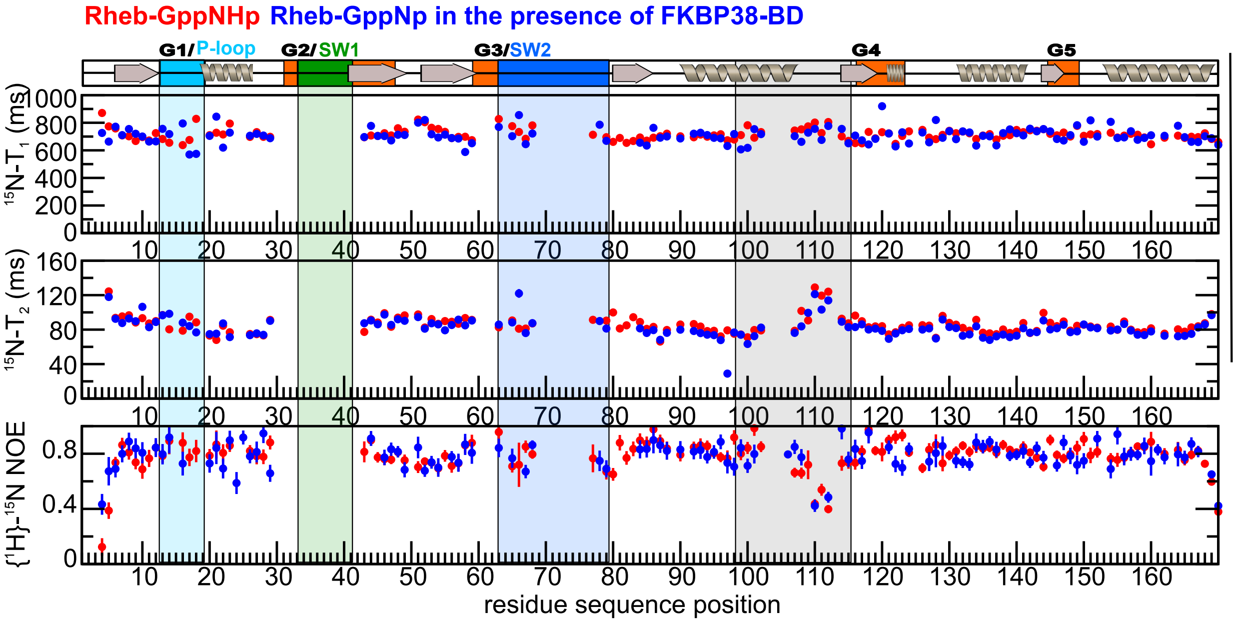

De Cicco et al.
SI Fig. S8

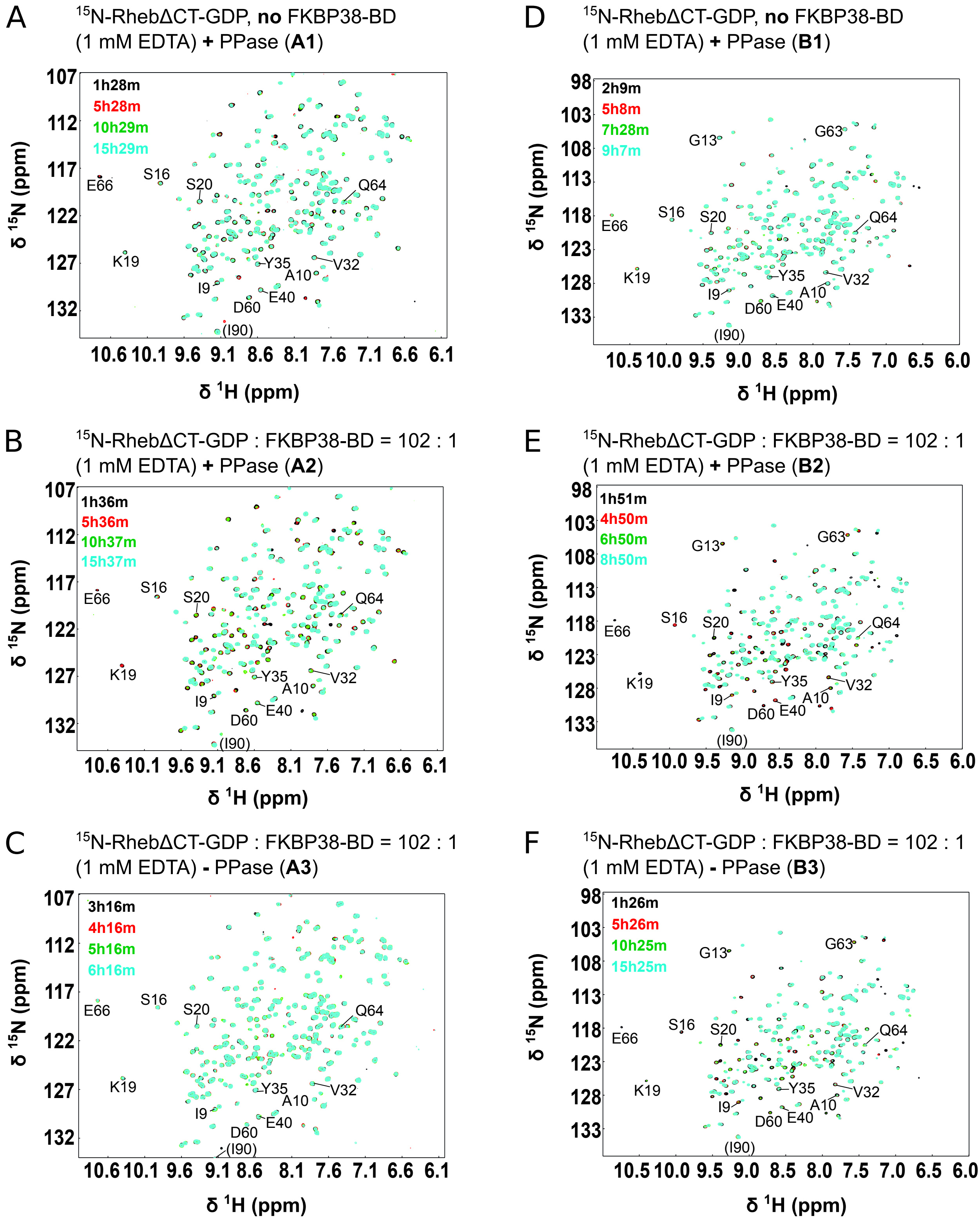

De Cicco et al.
SI Fig. S9

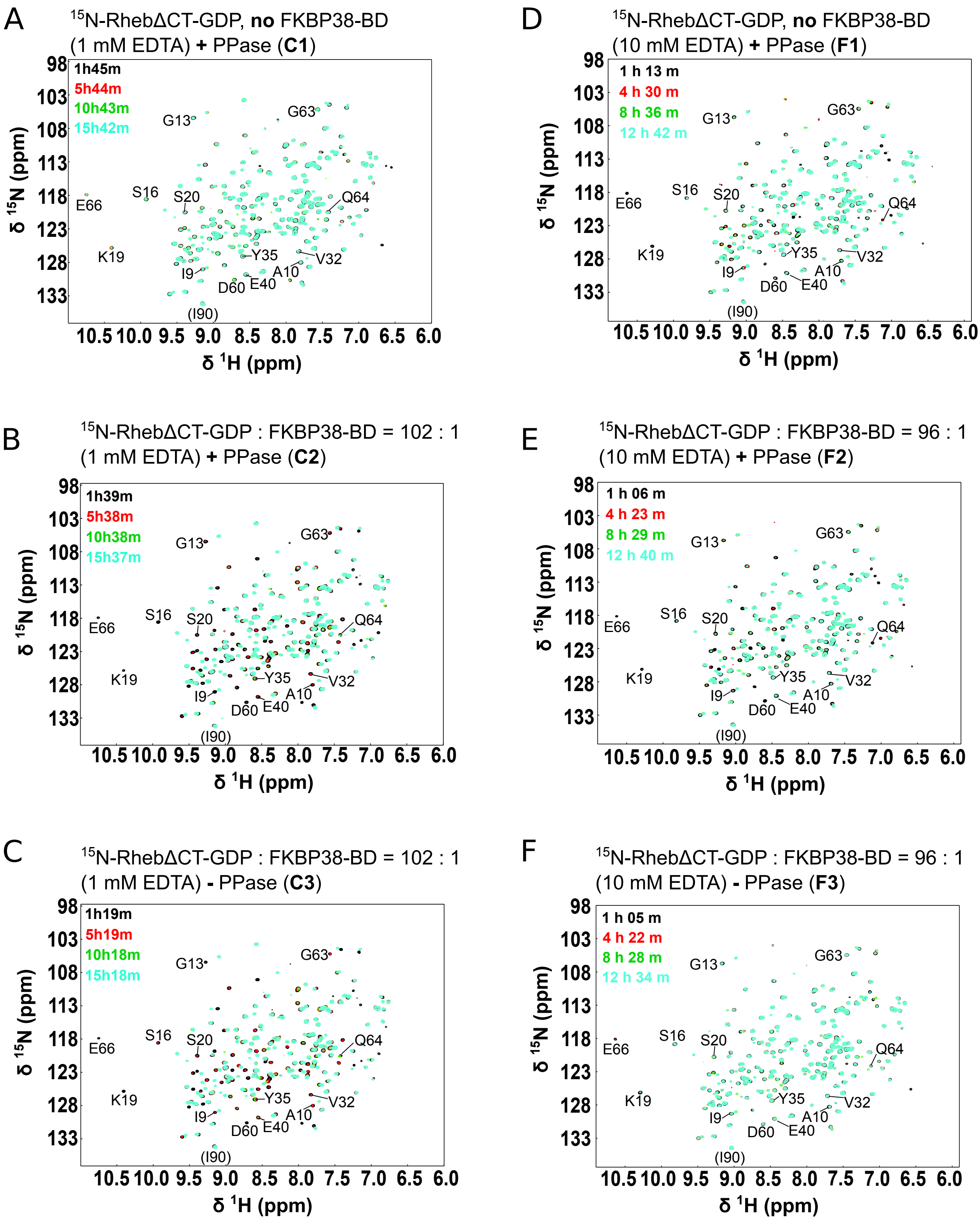

De Cicco et al.
SI Fig. S10

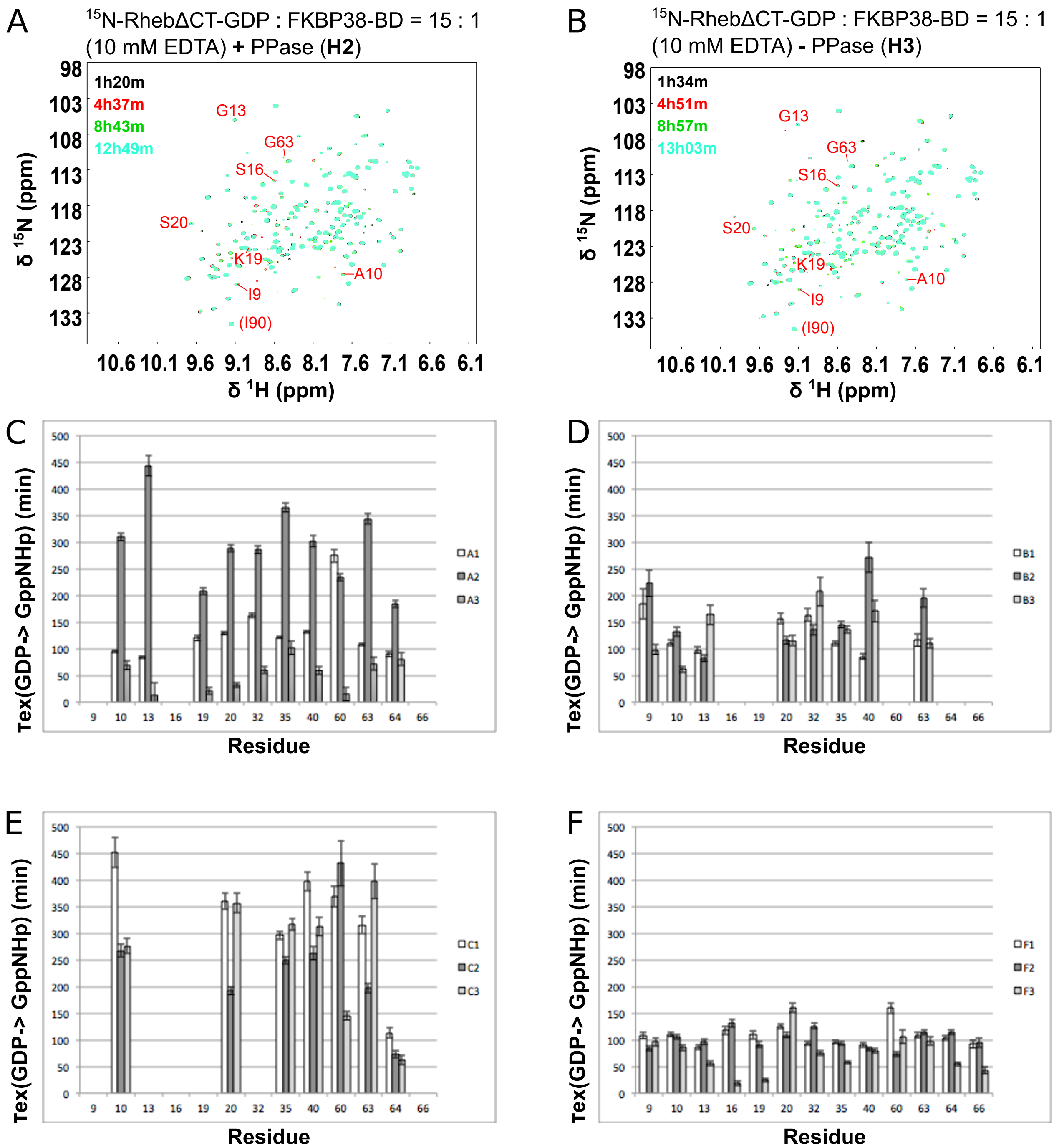

De Cicco et al.
SI Fig. S11

```
                         1        10        20        30        40        50        60
                         .        .         .         .         .         .         .
sp|Q15382|RHEB_HUMAN     MPQSKSRKIAILGYRSVGKSSLTIQFVEGQFVDSYDPTIENTFTKLITVNGQEYHLQLVD
sp|P01112|RASH_HUMAN     ...MTEYKLVVVGAGGVGKSALTIQLIQNHFVDEYDPTIEDSYRKQVVIDGETCLLDILD
sp|P60953|CDC42_HUMA     ...MQTIKCVVVGDGAVGKTCLLISYTTNKFPSEYVPTVFDNYAVTVMIGGEPYTLGLFD
consensus>50             ...m...K.v!vG.g.VGKs.LtIqfven.FvdeYdPT!e#.%.k.!.!nG#.y.Lql.D

                                  70        80        90       100       110       120
                                  .         .         .         .         .         .
sp|Q15382|RHEB_HUMAN     TAGQDEYSIFPQTYSIDINGYILVYSVTSIKSFEVIKVIHGKLLDMVGKVQIPIMLVGNK
sp|P01112|RASH_HUMAN     TAGQEEYSAMRDQYMRTGEGFLCVFAINNTKSFEDIHQYREQIKRVKDSDDVPMVLVGNK
sp|P60953|CDC42_HUMA     TAGQEDYDRLRPLSYPQTDVFLVCFSVVSPSSFENVKE.KWVPEITHHCPKTPFLLVGTQ
consensus>50             TAGQ##Ys.mrq.y..d.#g%l.v%s!.s.kSFEd!kq............qiP.mLVGnk

                                130       140       150       160         170
                                  .         .         .         .           .
sp|Q15382|RHEB_HUMAN     KDLHMERVISYEEGKALAESWNAAFLESSAKENQTAVDVFRRIILEAE..KM..DGAASQ
sp|P01112|RASH_HUMAN     CDL.AARTVESRQAQDLARSYGIPYIETSAKTRQGVEDAFYTLVREIRQHKL..RKLNPP
sp|P60953|CDC42_HUMA     IDLRDDPSTIEKLAKNKQKPITPETAEKLARDLKAVKYVECSALTQKGLKNVFDEAILAA
consensus>50             .DL..er.i...eakdla.s....f.E.sAke.q.v.dvf...i.#....km..d.....

                           180
                             .
sp|Q15382|RHEB_HUMAN     GKSSCSVM.......
sp|P01112|RASH_HUMAN     DESGPGCMSCKCVLS
sp|P60953|CDC42_HUMA     LEPPEPKKSRRCVLL
consensus>50             .es....ms..cvl.
```